Title

Novel and shared neoantigen derived from histone 3 variant H3.3K27M mutation for glioma T cell therapy.

Journal

The Journal of experimental medicine, 215(1)

ISSN

0022-1007

Authors

Chheda, Zinal S
Kohanbash, Gary
Okada, Kaori
et al.

Publication Date

2018

DOI

10.1084/jem.20171046

Peer reviewed

Novel and shared neoantigen derived from histone 3 variant H3.3K27M mutation for glioma T cell therapy

Zinal S. Chheda,[1]* Gary Kohanbash,[1,10]* Kaori Okada,[1] Naznin Jahan,[1] John Sidney,[4] Matteo Pecoraro,[5] Xinbo Yang,[6] Diego A. Carrera,[1] Kira M. Downey,[1] Shruti Shrivastav,[1] Shuming Liu,[1] Yi Lin,[1] Chetana Lagisetti,[9] Pavlina Chuntova,[1] Payal B. Watchmaker,[1] Sabine Mueller,[1] Ian F. Pollack,[10] Raja Rajalingam,[2] Angel M. Carcaboso,[11] Matthias Mann,[5] Alessandro Sette,[4] K. Christopher Garcia,[6,7,8] Yafei Hou,[1] and Hideho Okada[1,3,12]

[1]Department of Neurological Surgery, [2]Department of Surgery, Immunogenetics and Transplantation Laboratory, and [3]Cancer Immunotherapy Program, University of California, San Francisco, San Francisco, CA
[4]Center for Infectious Disease, Division of Vaccine Discovery, La Jolla Institute for Allergy and Immunology, La Jolla, CA
[5]Department of Proteomics and Signal Transduction, Max Planck Institute of Biochemistry, Martinsried, Germany
[6]Department of Molecular and Cellular Physiology, [7]Howard Hughes Medical Institute, and [8]Department of Structural Biology, Stanford University School of Medicine, Stanford, CA
[9]Department of Public Health, University of California, Berkeley, Berkeley, CA
[10]Department of Neurosurgery, University of Pittsburgh School of Medicine, Pittsburgh, PA
[11]Institut de Recerca Sant Joan de Deu, Barcelona, Spain
[12]The Parker Institute for Cancer Immunotherapy, San Francisco, CA

The median overall survival for children with diffuse intrinsic pontine glioma (DIPG) is less than one year. The majority of diffuse midline gliomas, including more than 70% of DIPGs, harbor an amino acid substitution from lysine (K) to methionine (M) at position 27 of histone 3 variant 3 (H3.3). From a $CD8^+$ T cell clone established by stimulation of HLA-$A2^+$ $CD8^+$ T cells with synthetic peptide encompassing the H3.3K27M mutation, complementary DNA for T cell receptor (TCR) α- and β-chains were cloned into a retroviral vector. TCR-transduced HLA-$A2^+$ T cells efficiently killed HLA-$A2^+$H3.3K27M$^+$ glioma cells in an antigen- and HLA-specific manner. Adoptive transfer of TCR-transduced T cells significantly suppressed the progression of glioma xenografts in mice. Alanine-scanning assays suggested the absence of known human proteins sharing the key amino acid residues required for recognition by the TCR, suggesting that the TCR could be safely used in patients. These data provide us with a strong basis for developing T cell–based therapy targeting this shared neoepitope.

INTRODUCTION

Malignant gliomas, including glioblastoma and diffuse midline glioma (DMG), are lethal brain tumors in both adults and children (Louis et al., 2016). Indeed, brain tumors are the leading cause of cancer-related mortality and morbidity in children (Brain Tumor Progress Review Group, 2000). Children with DIPG have 1-year progression-free survival rates of less than 25% and median overall survival of 9–10 months with current treatments (Kebudi and Cakir, 2013; Schroeder et al., 2014).

The concept of cancer immunotherapy is based on the notion that the human immune system can recognize cancer-derived antigens as "non-self." In recent cancer immunotherapy trials, life-threatening and fatal events were caused by on-target (Johnson et al., 2009; Morgan et al., 2010; Parkhurst et al., 2011) or off-target (Cameron et al., 2013; Morgan et al., 2013) cross-reactivity of T cells against normal cells. These observations underscore the need for expanding the list of available tumor-specific antigens, such as mutation-derived antigens (i.e., neoantigens), for safe and effective immunotherapy. Although the list of antigens that could be used for glioma immunotherapy has expanded over the last decade (Okada et al., 2009; Reardon et al., 2013), there are not many truly glioma-specific antigens, except for those derived from epidermal growth factor receptor vIII (EGFRvIII; Thorne et al., 2016) and mutant isocitrate dehydrogenase 1 (IDH1; Schumacher et al., 2014).

Recent genetic studies have revealed that malignant gliomas in children and young adults often show somatic missense mutations in the histone H3 variant 3.3 (H3.3; Schwartzentruber et al., 2012). A majority of DMG and more than 70% of DIPG cases (Khuong-Quang et al., 2012) harbor the amino acid substitution from lysine (K) to methionine (M) at position 27 of H3.3 (H3.3K27M mutation). H3.3K27M mutation in DMG results in a global reduction of H3K27me3, leading to suppression of targets of polycomb repressive complex 2 (PRC2), thereby causing aberrant gene

*Z.S. Chheda and G. Kohanbash contributed equally to this paper.

Correspondence to Hideho Okada: hideho.okada@ucsf.edu

The Rockefeller University Press
J. Exp. Med. 2018 Vol. 215 No. 1 141–157
https://doi.org/10.1084/jem.20171046

The Journal of Experimental Medicine

expression (Jones and Baker, 2014). Patients with H3.3K27M$^+$ DIPG generally have shorter survival times than those with nonmutated H3.3 (H3.3WT; Khuong-Quang et al., 2012).

We discuss herein the identification of an HLA-A*02:01-restricted CD8$^+$ CTL epitope encompassing the H3.3K27M mutation. Furthermore, we have cloned cDNA for TCR α- and β-chains derived from an H3.3K27M-specific CD8$^+$ T cell clone. The TCR binds to the HLA-A*02:01-peptide complex at excellent affinity levels, and HLA-A*02:01$^+$ donor-derived T cells transduced with the TCR recognize and lyse HLA-A*02:01$^+$ H3.3K27M$^+$ glioma cells in a mutation- and HLA-specific manner. Importantly, alanine scan assays demonstrated that there are no known human proteins that share the set of key amino acid residues for recognition by the TCR. Our data strongly support development of vaccine- and TCR-transduced T cell–based immunotherapy strategies in patients with H3.3K27M$^+$ gliomas.

RESULTS

The H3.3K27M peptide binds to HLA-A*02:01

Using the NetMHC 3.4 server (http://www.cbs.dtu.dk/services/NetMHC/), an artificial neural network–based bioinformatic tool for predicting the binding of peptides to HLA class I MHC molecules, we predicted that a decamer (10-mer) peptide H3.3K27M$_{26–35}$, encompassing residues 26–35 of the H3.3 sequence and including the K27M mutation (H3.3K27M peptide), would bind HLA-A*02:01 with high affinity. Interestingly, the nonmutant counterpart H3.3WT$_{26–35}$ was not predicted to have high affinity for HLA-A*02:01 (hereafter H3.3WT peptide; Table 1). To confirm these predictions, we measured the binding of synthetic peptides to purified HLA-A*02:01 using a competitive inhibition assay. Consistent with the NetMHC 3.4 predictions, we found that the H3.3K27M peptide, but not H3.3WT, bound HLA-A*02:01 with high affinity (Table 1). We also extended our binding analysis to HLA-A*02:02, A*02:03, A*02:06, A*02:07, and A*02:17 and found that the H3.3K27M peptide weakly bound to A*02:03 (half-maximal inhibitory concentration [IC$_{50}$] 747 nM), but none of the other evaluated HLA-A2 subtypes did (Table S1).

The H3.3K27M peptide induces specific T cell responses in HLA-A2$^+$ patients with H3.3K27M$^+$ glioma and leads to isolation of high tetramer–binding CD8$^+$ T cell clones

To evaluate whether the H3.3K27M epitope induces an antigen-specific response in peripheral blood mononuclear cells (PBMCs) of DIPG patients, we stimulated PBMC samples derived from three HLA-A*02:01$^+$ DIPG patients and three HLA-A*02:01$^+$ healthy donors in vitro with H3.3WT, H3.3K27M, influenza matrix protein M1$_{58–66}$ peptide (hereafter flu peptide) or without peptide for 1 wk and performed IFN-γ ELISPOT assays after co-culture with T2 cells loaded with H3.3WT, H3.3K27M, or flu peptide. In all three patients but none of healthy donors, PBMCs stimulated with the H3.3K27M peptide showed antigen-specific increases of IFN-γ spots when co-cultured with T2 cells loaded with H3.3K27M peptide (Fig. 1 A). On the other hand, PBMCs stimulated with H3.3WT demonstrated only background or significantly lower levels of IFN-γ compared with H3.3K27M-stimulated PBMCs. Although PBMCs from patient 1 demonstrated higher background levels than those of other donors, H3.3K27M-stimulated PBMCs showed significantly higher levels of IFN-γ production upon co-culture with H3.3K27M-loaded T2 cells compared with other conditions. PBMCs stimulated with the flu peptide served as a positive control in this assay. These results suggest that H3.3K27M$^+$ gliomas may elicit spontaneous CD8$^+$ T cell responses in HLA-A*02:01$^+$ patients, but the level of the responses is not sufficient to prevent tumor development.

Next, we stimulated HLA-A*02:01$^+$ healthy donor–derived PBMCs with synthetic H3.3K27M peptide in vitro for four weekly cycles and evaluated the induction of CD8$^+$ T cells capable of binding to the HLA-A*02:01-H3.3K27M$_{26–35}$ tetramer. As demonstrated in Fig. 1 B, we found that >60% of CD8$^+$ T cells bound to the tetramer. Furthermore, a subpopulation of the CD8$^+$tetramer$^+$ T cells in the culture showed distinctively higher levels of binding to the tetramer (tetramer^{high} population; 2.4% of CD8$^+$ cells; Fig. 1 B). Among several CD8$^+$ T cell clones established by limiting dilution of the tetramer^{high} CTL subpopulation, we selected clone 1H5 for subsequent studies because of its excellent tetramer reactivity (Fig. 1 C). Clone 1H5 also demonstrated a peptide dose–dependent increase of IFN-γ production when stimulated by HLA-A*02:01$^+$ T2 cells loaded with mutant H3.3K27M peptide, but not the H3.3WT peptide (Fig. 1 D).

The H3.3K27M peptide is presented as an HLA-A*02:01$^+$-binding epitope by glioma cells transfected with H3.3K27M cDNA

To investigate whether the bioinformatically predicted H3.3K27M$_{26–35}$ peptide is produced and presented by the HLA machinery in HLA-A*02:01$^+$ H3.3K27M$^+$ glioma cells, we used a recently developed mass spectrometry (MS)-based method for the direct identification of HLA

Table 1. **HLA-A*02:01-binding affinity of H3.3K27M$_{26–35}$ mutant versus H3.3WT$_{26–35}$ nonmutant peptides**

Peptide	Amino acid sequence	Predicted affinity (nM)/log score	Actual affinity (nM)
H3.3K27M	R<u>M</u>SAPSTGGV	285/0.477	151
H3.3WT	R<u>K</u>SAPSTGGV	22,651/0.073	>38,687

The predicted binding affinity was determined using the NetMHC3.4 server. Peptides were tested at six different concentrations covering a 100,000-fold dose range in three or more independent assays. The underlined letter suggests the position of mutation in the peptide epitope.

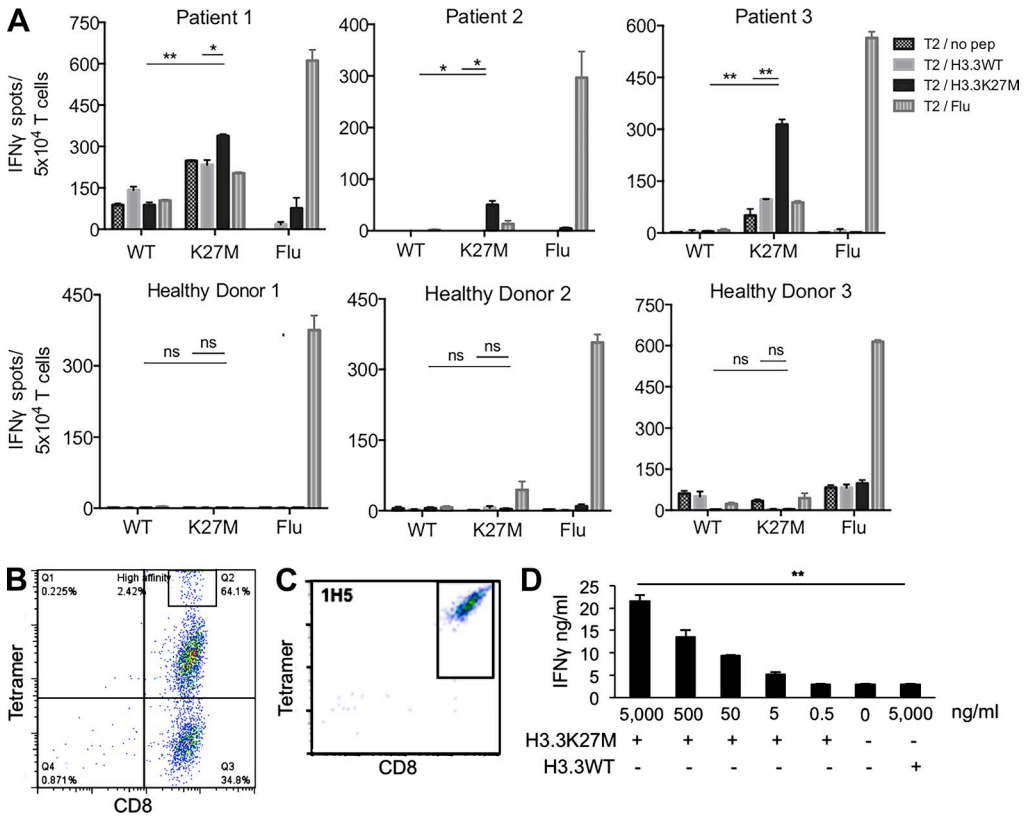

Figure 1. **H3.3K27M peptide induces T cell responses in DIPG patients and led to isolation of H3.3K27M–specific CTL clones from HLA-A2$^+$ donor PBMCs. (A)** Patient-derived and healthy donor-derived PBMCs were stimulated with H3.3WT, H3.3K27M, and flu peptide or without peptide and co-cultured with T2 cells pulsed with H3.3WT, H3.3K27M, and flu peptide or without peptide. Numbers of IFN-γ spots per 5 × 10^4 T cells generated in each stimulation condition. Counts shown are normalized to no-peptide stimulation control. Bars and error bars represent median and SD, respectively, for IFN-γ spots per 5 × 10^4 T cells observed in each stimulation condition. $n = 3$ in each group. Experiment was conducted once. *, $P < 0.05$; **, $P < 0.01$ by Student's t test comparing H3.3WT and H3.3K27M stimulation groups. ns, not significant. **(B)** HLA-A*02:01$^+$ healthy donor-derived PBMCs were stimulated in vitro with H3.3K27M peptide and evaluated for reactivity against HLA-A*02:01-H3.3K27M-specific tetramer and anti-CD8 mAb using flow cytometry (gated on live lymphocytes). Tetramer$^+$ gate was based on control T cells. Tetramer^{high} population (2.42%) represented the high-affinity CTL population. **(C)** CTL clones were generated by flow-sorting followed by limiting dilution cloning of tetramer^{high} CD8$^+$ T cells. The clone 1H5 was chosen for further investigation based on its excellent tetramer reactivity. The dot plot demonstrates that the clone 1H5 retains the reactivity levels to the HLA-A*0201/H3.3K27M-specific tetramer. **(D)** Bar graph representing IFN-γ production from the T cell clone 1H5 measured by ELISA after co-culture with T2 cells pulsed with H3.3K27M peptide at titrating concentrations or with H3.3WT peptide (5 µg/ml). Data represent two independent experiments with similar results. Bars and error bars represent median and SD, respectively, for IFN-γ production levels. **, $P < 0.01$ using Student's t tests comparing 5 µg/ml H3.3WT and H3.3K27M peptide concentrations.

class I–binding peptides (Bassani-Sternberg et al., 2015). We purified HLA class I–binding peptides from HLA-A*02:01$^+$H3.3K27M$^-$ U87MG glioma cells stably transduced with cDNA encoding H3.3K27M (U87H3.3K27M), H3.3WT (U87H3.3WT), or parental U87MG cells (Table S3) and analyzed them by LC-MS/MS using a quadrupole Orbitrap mass spectrometer. To specifically identify the H3.3K27M$_{26–35}$ peptide, we added a fixed amount of a synthetic version of the H3.3K27M$_{26–35}$ 10-mer to each sample containing a substitution of arginine at position 1 with the heavy counterpart (13C6 15N4 arginine), thus introducing a 10.0083-D mass difference. With this approach, the heavy labeled peptide was readily sequenced and identified because of its higher abundance during LC-MS/MS analysis. Because both the heavy and light peptides elute at the same time from the chromatographic column and differ exclusively in the introduced mass change, it was possible to confidently identify the endogenous peptide even at extremely low concentrations and in the absence of an MS/MS spectrum. After recalibration in MaxQuant, we detected two coeluting isotope patterns with mass-to-charge ratios (m/z) of 494.7420 and 489.7394 at 27.74 min of chromatographic separation in U87H3.3K27M glioma cells (Fig. 2 A). This was compatible with the predicted values for both heavy and endogenous H3.3K27M$_{26–35}$ peptides in their oxidized forms (494.7414 and 489.7373, respectively) with a relative mass difference of 10.0052 D. The elution peak corresponding to the heavy peptide was selected multiple times for sequencing, and its

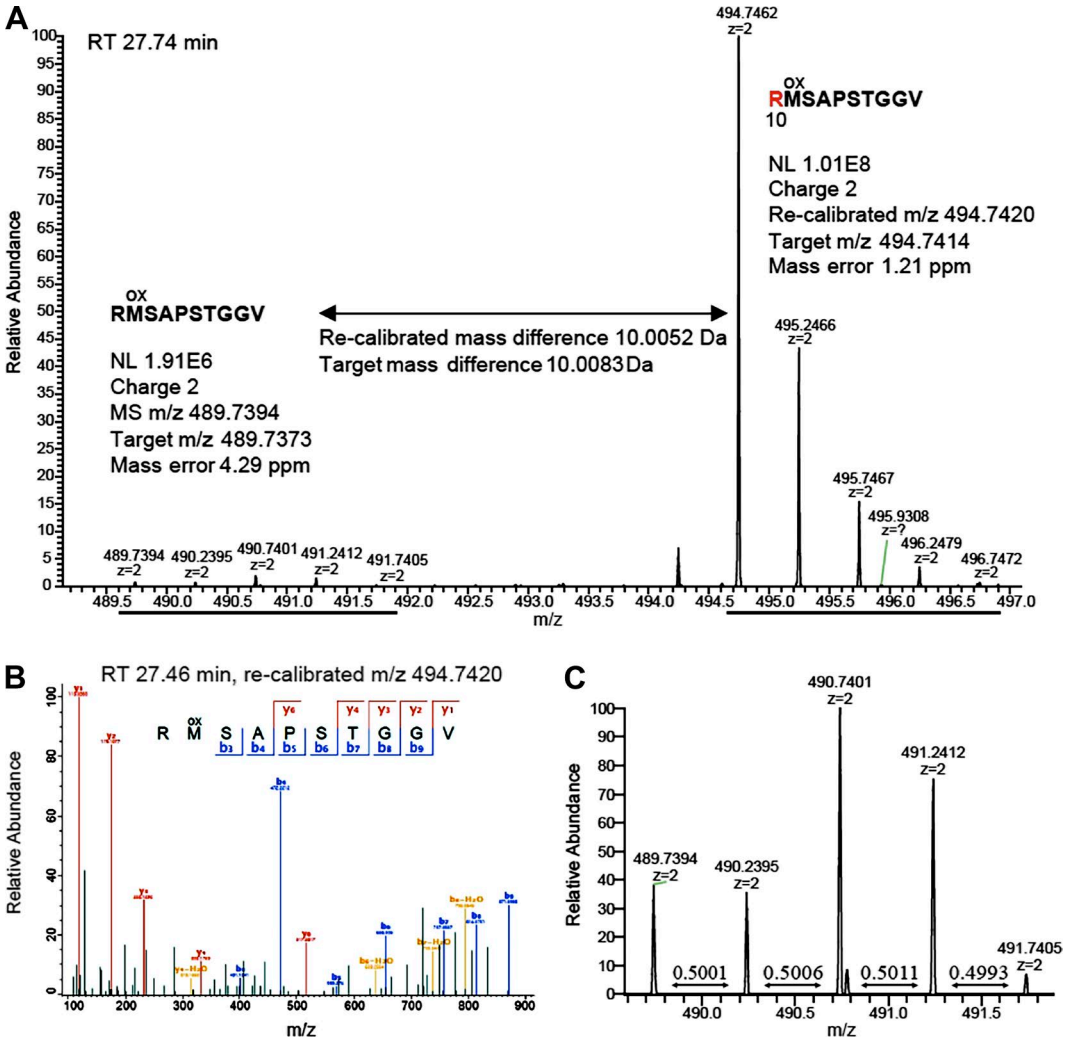

Figure 2. **The H3.3K27M peptide is detectable by LC-MS/MS in the HLA class I immunopeptidome of glioma cells bearing the H3.3K27M mutation.** HLA class I peptides were biochemically purified from U87H3.3K27M glioma cells and analyzed by LC-MS/MS with a synthetic heavy version of the H3.3K27M peptide as the reference. **(A)** U87H3.3K27M HLA class I immunopeptidome shows two coeluting isotope patterns corresponding to the target *m/z* and mass difference of the oxidized forms of the heavy and the endogenous H3.3K27M peptides. **(B)** Fragmentation spectrum of the heavy peak, showing identification of the oxidized heavy H3.3K27M peptide. **(C)** Zoom-in of the light isotope pattern shows *m/z* values and distances between peaks as expected from the endogenous H3.3K27M peptide. This experiment was conducted once.

fragmentation spectrum was unequivocally identified as the oxidized form of the heavy H3.3K27M (Andromeda identification score 124.23; Fig. 2 B). The putative light isotope pattern presented correct *m/z* values for each of its isotopic peaks (Fig. 2 C). Moreover, this isotope pattern was detectable exclusively in U87H3.3K27M cells but not in either parental U87 or U87H3.3WT cells (not depicted). The modification observed in both peptides is caused by oxidation of the methionine residue during experimental sample preparation and therefore does not reflect the state of the peptide in vivo (Lagerwerf et al., 1996). Together, these observations demonstrate that the H3.3K27M$_{26–35}$ epitope peptide is naturally produced and presented by HLA class I on the surface of glioma cells transfected with H3.3K27M cDNA.

Human T cells transduced with retroviral vector encoding H3.3K27M-specific TCR demonstrate H3.3K27M-specific CTL reactivity

We isolated full-length cDNA for α- and β-chains of TCR from the clone 1H5, optimized the codon usage, and cloned them into a TCR retroviral vector system, which incorporates siRNA targeting constant regions of the endogenous TCR α- and β-chains to avoid mispairing between endogenous and transgene TCR chains (Fig. 3 A; Okamoto et al., 2009, 2012). To evaluate the function of the transgene TCR, especially in relation to coexpression of CD8, we transduced the Jurkat T cell clone 76 (J76CD8$^-$), which is deficient of endogenous CD8 as well as TCR α- and β-chains (Heemskerk et al., 2003), and CD8-transfected Jurkat T cell clone 76 (J76CD8$^+$)

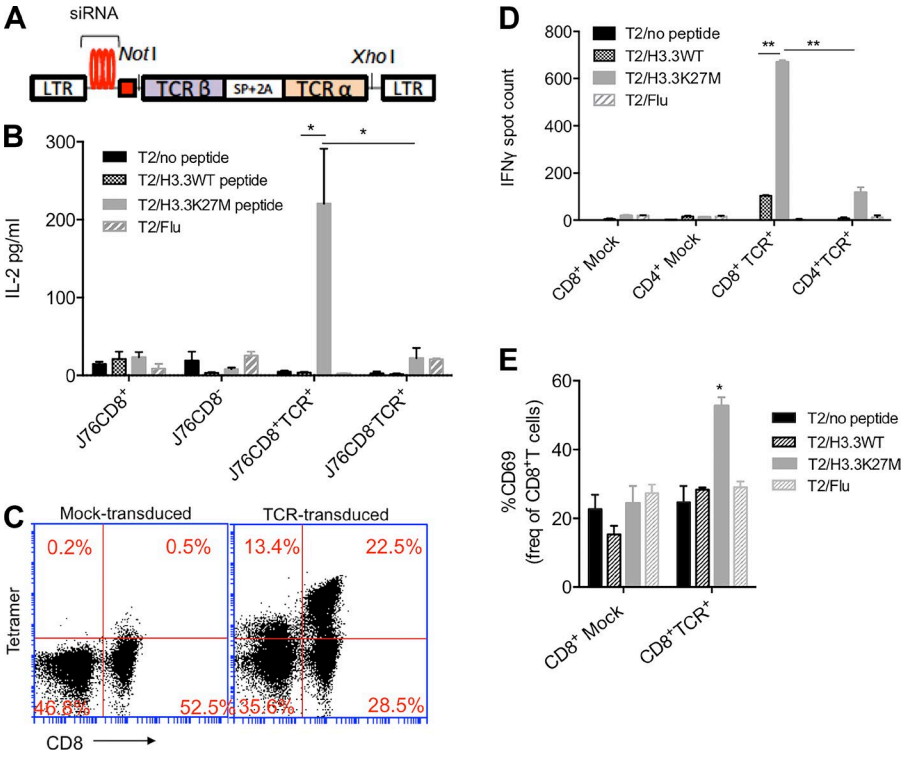

Figure 3. **Cloning of cDNA for the H3.3K27M-specific TCR and construction of a retroviral vector for efficient transduction of human T cells. (A)** Schema of the TCR retroviral vector design. Synthesized TCR cDNA fragments derived from the $CD8^+$ T cell clone 1H5 were inserted into the NotI/XhoI site of Takara siTCR vector plasmid together with the Kozak sequence, spacer sequence (SP), and P2A sequence. **(B)** T2 cells loaded with or without H3.3K27M, H3.3WT, or irrelevant influenza matrix $M1_{58-66}$ flu peptide (10 µg/ml) were co-cultured with either control or TCR-transduced Jurkat76$CD8^+$ or Jurkat76$CD8^-$ cells in a 1:1 ratio and assessed for IL-2 production by ELISA. Data represent three independent experiments with similar results. Bars and error bars represent median and SD, respectively, for IL-2 levels (n = 3 in each group). *, $P < 0.05$ by Student's t test compared with each of the other groups. **(C)** Human PBMCs were transduced with the retroviral TCR vector, and $CD3^+$ T cells were evaluated for transduction efficiency in $CD8^+$ and $CD8^-$ T cell populations by the specific tetramer. Of the 51% of $CD8^+$ T cells, 22.5% were tetramer$^+$, and of 49% of $CD4^+$ T cells, 13.4% were tetramer$^+$. **(D)** TCR-transduced or mock-transduced primary human $CD4^+$ or $CD8^+$ T cells were co-cultured with T2 cells loaded with H3.3K27M, H3.3WT, or flu peptide in a 1:1 ratio overnight for IFN-γ ELISPOT. Bars and error bars represent median and SD, respectively, for IFN-γ spot counts/5×10^4 T cells in triplicate. **, $P < 0.01$ by Student's t test comparing TCR-transduced $CD8^+$ versus TCR-transduced $CD4^+$ T cells, and H3.3WT versus H3.3K27M peptide-stimulated groups for TCR-transduced $CD8^+$ T cells. Data represent two independent experiments with similar results. **(E)** TCR-transduced or mock-transduced $CD8^+$ T cells were co-cultured with T2 cells pulsed with H3.3WT, H3.3K27M, or flu peptide in a 1:1 ratio, followed by evaluation of CD69 expression. Bars and error bars represent median and SD, respectively, for percentage $CD69^+$ cells among $CD8^+$ T cells (n = 3 in each group). Data represent two independent experiments with similar results. *, $P < 0.05$ by Student's t test compared with each of the other groups.

with the TCR vector. The TCR-transduced J76$CD8^{+/-}$ cells were then co-cultured with T2 cells pulsed with H3.3WT, H3.3K27M, or irrelevant flu peptide. TCR-transduced J76$CD8^+$ cells produced significantly higher levels of IL-2 in response to H3.3K27M peptide compared with all the other groups, indicating H3.3K27M-specific and CD8-dependent reactivity of the TCR (Fig. 3 B).

Next, we transduced primary human T cells with the TCR and achieved >40% transduction efficiency in $CD8^+$ T cells and ~20% in $CD4^+$ T cells based on tetramer staining, suggesting that the CD8 coreceptor is important for efficient expression of the TCR (Fig. 3 C). To evaluate the functionality of the TCR in human primary T cells as well as the requirement of the CD8 coreceptor for functional response, $CD4^+$ T cells and $CD8^+$ T cells were simultaneously transduced with the TCR and co-cultured with T2 cells pulsed with H3.3K27M, H3.3WT, or flu peptide, and IFN-γ production was evaluated by ELISPOT (Fig. 3 D). TCR-transduced $CD8^+$ T cells produced significantly higher numbers of IFN-γ spots than TCR-transduced $CD4^+$ T cells upon stimulation with H3.3K27M peptide. Moreover, the response of TCR-transduced $CD8^+$ T cells was specific to H3.3K27M peptide, as these cells produced significantly higher numbers of IFN-γ spots in response to H3.3K27M peptide compared with H3.3WT, flu peptide, or no peptide (Fig. 3 D). However, although not at statistically significant levels, we observed a trend that TCR-transduced $CD8^+$ T cells produced increased numbers of IFN-γ spots compared with mock-transduced $CD8^+$ T cells against T2 cells loaded with H3.3WT peptide ($P = 0.254$). Although the concentration of the peptide was clearly supraphysiological (10 µg/ml), this observation should remind us of a theoretical possibility of off-tumor reactivity.

We also observed significant up-regulation of the T cell activation marker, CD69 (Werfel et al., 1997), on TCR-transduced $CD8^+$ T cells, but not mock-transduced T cells stimulated with the H3.3K27M peptide but not H3.3WT or an irrelevant flu peptide (Fig. 3 E). Mock-transduced T cells were prepared by the same activation method as TCR-transduced T cells using anti-CD3 antibody and RetroNectin as detailed in Materials and methods.

Alanine scanning data suggest the absence of known human proteins that share the key immunogenic amino acid residues of the H3.3K27M epitope

To ensure the specificity and safety of the H3.3K27M-targeting approach, it is essential to determine the key amino acid residues in the H3.3K27M epitope that are responsible for the TCR reactivity. This allows the prediction and assessment of cross-reactivity to other epitopes derived from proteins present in normal cells. To this end, we performed alanine-scanning mutagenesis of the H3.3K27M epitope by introducing single alanine mutations (10 in total) at every position within the H3.3K27M decamer epitope. Hence, we prepared 10 unique synthetic peptides that each contained a specific amino acid substitution with alanine (A1–A10) and evaluated whether the substitution alters the stability of peptide binding to HLA-A*02:01 (Fig. 4 A). When the binding was diminished by the substitution compared with the H3.3K27M epitope, it suggests that the substituted residue was critical for HLA-A*02:01 binding of the epitope. Accordingly, substitutions at position 2 and the C terminus were associated with >20-fold reductions in binding capacity, consistent with these positions being canonical HLA-A*02:01 primary anchors. Reductions in the 10–20-fold range were also noted in positions 1, 4, 6, 7, and 9, suggesting that they may also act as secondary MHC contacts.

Next, we evaluated IL-2 production as the readout for the functionality of TCR-transduced cells when co-cultured with T2 cells loaded with each of the altered peptides (Fig. 4 B). Amino acids for which substitutions result in diminished IL-2 production are critical for recognition by the TCR. Both HLA binding affinity (Fig. 4 A) and TCR reactivity as determined by IL-2 production (Fig. 4 B) consistently showed that amino acids at positions 1, 2, 4, 6, 7, 8, 9, and 10 are critical for TCR recognition and function. Using NCBI BLAST 2.7.0, we queried for "RMXAXSTGGV" (residues 1, 2, 4, 6, 7, 8, 9, and 10) against the Homo Sapiens Protein Data Bank Proteins database and found no known human proteins that contain the same amino acid residues. We extended our search to find proteins with amino acid motifs that are homologous to the key amino acid residues (Table S2). Not surprisingly, relatively high homology was found in histone H3 family proteins and PRC2, but not other proteins. Based on the alanine scanning data, these proteins are not likely to be targeted by the TCR.

The H3.3K27M-specific TCR does not recognize the nonmutated, deiminated H3.3K27M epitope or H3.1-derived K27M peptide

Consistent with our data in Figs. 1 and 3, the H3.3WT peptide does not bind or elicit IL-2 production by the TCR (Fig. 4). The natural process of deimination can convert histone arginine to citrulline, including the arginine residue within the H3.3K27M epitope (i.e., deimination; Cuthbert et al., 2004). Therefore, it is useful to determine whether deimination can affect the immunogenicity of the H3.3K27M epitope.

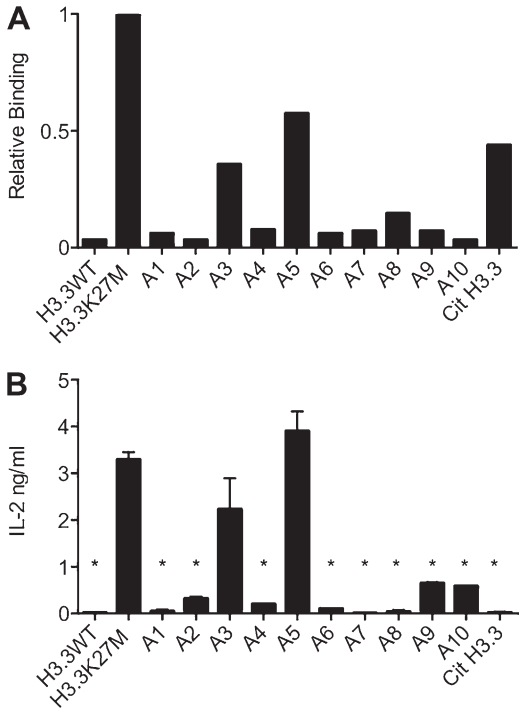

Figure 4. **Alanine scanning mutagenesis determines key amino acid residues in the H3.3K27M epitope required for TCR recognition.** Single alanine mutations (10 in total) were introduced at every amino acid residue within the H3.3K27M epitope (10-mer). Hence, 10 synthetic peptides each containing the specific substitution with alanine (A1–A3 and A5–A10) or valine (A4) were evaluated. In addition, synthetic peptides designed for nonmutated H3.3WT peptide and citrullinated H3.3K27M (Cit H3.3; i.e., the first amino acid of the H3.3K27M epitope was replaced by citrulline) were evaluated. **(A)** Relative HLA-A*0201 binding affinity of each peptide to that of H3.3K27M was determined by cell-free binding assay. This experiment was performed once. **(B)** J.RT3-T3.5 cells were transduced with H3.3K27M-specific TCR and evaluated for IL-2 production in response to T2 cells loaded with each peptide (10 µg/ml). Each group was assayed in triplicate. Bars and error bars represent median and SD, respectively, for IL-2 production levels. Data represent two independent experiments with similar results. *, $P < 0.05$ was calculated using Student's *t* test comparing each peptide with the mutant H3.3.

To this end, we evaluated whether the H3.3K27M-specific TCR is reactive to the deiminated H3.3K27M epitope using a synthetic peptide in which the arginine residue of the H3.3K27M epitope is replaced by citrulline (Cit H3.3; Fig. 4, A and B). Although the Cit H3.3 peptide partially retains its affinity to HLA-A*02:01 (Fig. 4 A), it completely abrogates IL-2 production by TCR-transduced Jurkat cells, indicating that the TCR does not recognize the Cit H3.3 peptide.

A subpopulation of glioma patients bear the K27M mutation in H3.1 (a homologue of H3.3; Jones and Baker, 2014). H3.1K27M mutations are found in >20% of DIPG and 5% of DMG cases and are strongly associated with younger age (Jones and Baker, 2014). The amino acid sequences encompassing the K27M mutation in H3.1 and H3.3 are similar.

Compared with the H3.3K27M epitope, the corresponding portion of H3.1 has only one amino acid substitution at the sixth position in the 10-mer peptide and is therefore identical to the peptide A6 in the alanine scanning. Both binding (Fig. 4 A) and IL-2 production (Fig. 4 B) were abrogated in the case of A6, suggesting that patients with the H3.1K27M mutation but without the H3.3K27M mutation are not eligible for prospective TCR-transduced adoptive transfer therapy.

Characterization of affinity and functional avidity of the TCR

To determine the affinity of the TCR with H3.3K27M -HLA-A2 complex, we performed surface plasmon resonance (SPR) assays using recombinant TCR and the H3.3K27M-HLA-A2 complex, which was produced by in vitro folding from bacterial inclusion bodies. As shown in Fig. 5 (A and B), we obtained a dissociation constant (K_D) of 2.9 µM. Notably, this level of affinity is substantially higher than that of most TCRs directed against cancer antigens and is comparable to that of well-characterized TCRs against infectious pathogen-derived peptides (Aleksic et al., 2012).

To evaluate the functional avidity of the TCR, we determined the peptide concentration required to induce a half-maximal response (EC_{50}) per IFN-γ production by TCR-transduced $CD8^+$ and $CD4^+$ T cells obtained from three healthy HLA-A*02:01$^+$ donors. We determined the EC_{50} of TCR-transduced $CD8^+$ T cells to be between 10^{-8} and 10^{-9} M based on IFN-γ ELISPOT assay with T2 cells loaded with titrating doses of the H3.3K27M peptide (Fig. 5 C). Notably, TCR-transduced $CD4^+$ T cells showed much lower numbers of IFN-γ spots, suggesting a requirement of CD8 coreceptor for the functional response. The response of TCR-transduced $CD8^+$ T cells was specific to H3.3K27M peptide presented on HLA-A2, as demonstrated by the lack of response with T2 cells loaded with flu peptide (10 µg/ml) and HLA-A2–negative HSJD-DIPG-019 cells loaded with H3.3K27M peptide (10 µg/ml; Fig. 5 D). However, as we also noted in the dataset in Fig. 3 D, TCR-transduced $CD8^+$ T cells produced modest numbers of IFN-γ spots against T2 cells loaded with 10 µg/ml H3.3WT peptide (P = 0.1000 compared with the group of T2 cells with no peptide).

TCR-transduced T cells specifically lyse H3.3K27M$^+$HLA-A2$^+$ glioma cells in vitro

It is essential to demonstrate that TCR-transduced T cells are able to recognize the H3.3K27M epitope that is endogenously expressed in glioma cells and lyse H3.3K27M$^+$HLA-A*02:01$^+$ glioma cells. To this end, we evaluated cytotoxic activity of TCR-transduced T cells against three H3.3K27M$^+$ DIPG cell lines, HLA-A*02:01$^+$ HSJD-DIPG-017, HLA-A*02:01$^+$ HSJD-DIPG-021, and HLA-A*02:01^{neg} HSJD-DIPG-019, using lactate dehydrogenase (LDH) detection-based cytotoxicity assay (Table S3). Although both TCR-transduced and mock-transduced T cells were similarly activated, only TCR-transduced T cells lysed HLA-A*02:01$^+$ HSJD-DIPG-017 and HSJD-DIPG-021 cells (Fig. 6, A and B). The observed lysis was dependent on HLA-A*02:01, as TCR-transduced T cells were not able to lyse HSJD-DIPG-019 cells, even in the presence of exogenously

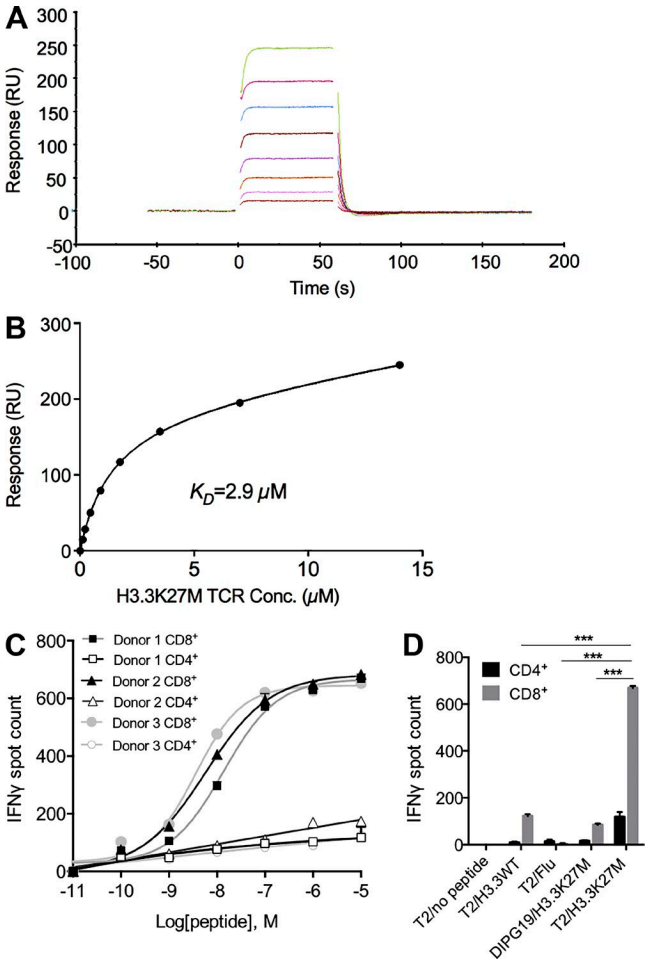

Figure 5. **Evaluation of TCR avidity to the HLA-A2–peptide complex. (A and B)** SPR analysis on the binding of the TCR and H3.3K27M-HLA-A2. (A) H3.3K27M TCR at concentrations of 14, 7, 3.5, 1.75, 0.9, 0.45, 0.23, 0.12, and 0 µM was injected over immobilized H3.3K27M-HLA-A2 (500 resonance units [RU]). (B) Fitted curve for equilibrium binding that resulted in a K_D of 2.9 µM. Data represent two independent experiments with similar results. **(C)** T2 cells (5 × 10^4/well) loaded with titrating concentrations of the H3.3K27M peptide were co-cultured with TCR-transduced $CD4^+$ or $CD8^+$ T cells derived from three donors (5 × 10^4/well) and assessed by IFN-γ ELISPOT. The EC_{50} of the peptide was calculated using nonlinear regression analysis. Each experiment was performed in triplicate, and data represent two independent experiments with similar results. **(D)** T2 cells were pulsed with 10 µg/ml H3.3WT, H3.3K27M, flu peptide, or no peptide, and HLA-A2^{neg}H3.3K27M$^+$HSJD-DIPG019 cells were pulsed with 10 µg/ml H3.3K27M peptide. These cells were co-cultured with $CD4^+$ or $CD8^+$ TCR-transduced T cells and assessed by IFN-γ ELISPOT. Bars and error bars represent median and SD, respectively, for IFN-γ spots. Data represent two independent experiments with similar results. Experiments were performed in triplicate. ***, P < 0.001 by Student's *t* test comparing the T2/H3.3K27M group with all the other stimulation conditions for $CD8^+$ T cell groups.

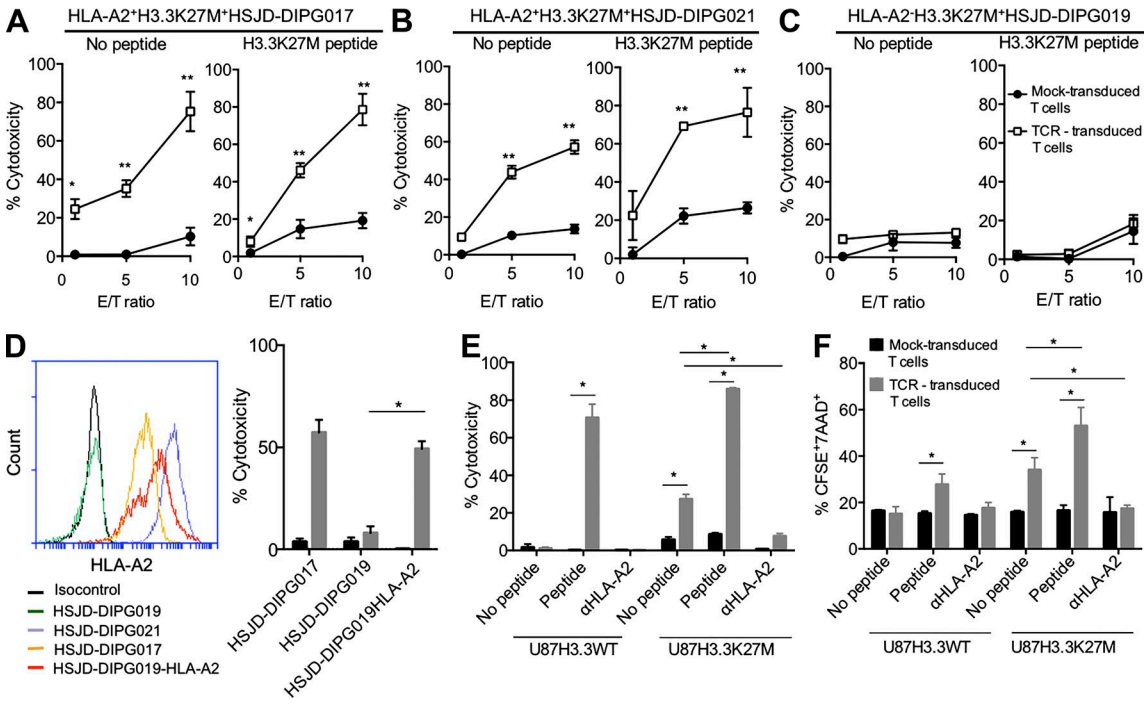

Figure 6. **TCR-transduced T cells lyse H3.3K27M$^+$HLA-A2$^+$ glioma cells in an HLA-A*0201- and H3.3K27M-dependent manner. (A–E)** Cytotoxicity of TCR-transduced T cells was evaluated by LDH cytotoxicity assay. Exogenous, synthetic H3.3K27M peptide (10 µg/ml) was added as a positive control group for TCR reactivity for each cell line. HLA-A2 blocking antibody was added in some experiments to determine HLA-A2–dependent TCR reactivity. (A–C) TCR-transduced or mock-transduced T cells were co-cultured with H3.3K27M$^+$HLA-A*0201$^+$ HSJD-DIPG-017 cells (A), H3.3K27M$^+$HLA-A*0201$^+$HSJD-DIPG-021 cells (B), or control H3.3K27M$^+$HLA-A*0201^{neg} HSJD-DIPG-019 cells (C) at an E/T ratio of 1, 5, and 10 for 24 h. *, $P < 0.05$; **, $P < 0.01$ based on Student's *t* test comparing TCR-transduced T cells with mock-transduced T cells. Each group was assessed in triplicate. Data represent two independent experiments with similar results. (D) HLA-A*0201-negative HSJD-DIPG-019 cells were stably transduced with lentiviral vector encoding HLA-A*0201 and evaluated for HLA-A2 expression by flow cytometry along with other cell lines. TCR-transduced or mock-transduced T cells were co-cultured with DIPG017, DIPG019, or DIPG-019-HLA-A2$^+$ cells at an E/T ratio of 5, and cytotoxicity was measured by LDH assay. Bars and error bars represent median and SD, respectively, for specific percentage cytotoxicity. *, $P < 0.05$ based on Student's *t* test. Each group was assessed in triplicate, and data represent two independent experiments with similar results. (E) TCR-transduced or control T cells were co-cultured with HLA-A*0201$^+$ U87H3.3K27M cells or U87H3.3WT cells at an E/T ratio of 5. Each group was assessed in triplicate. Data represent three independent experiments with similar results. *, $P < 0.05$ based on Student's *t* test. **(F)** CFSE-labeled target cells were co-cultured with TCR-transduced or control T cells with or without exogenous peptide at an E/T ratio of 5. After 24-h incubation, cells were stained with 7-AAD. %CFSE$^+$7-AAD$^+$ cells indicated specific percent cytotoxicity. Each group was assessed in triplicate. Data represent two independent experiments with similar results. *, $P < 0.05$ based on Student's *t* test.

added H3.3K27M peptide (Fig. 6 C). After stable transduction with *HLA-A*02:01*, HSJD-DIPG019 cells became susceptible to the cytotoxic effect of the TCR-transduced T cells (Fig. 6 D), indicating HLA-A*02:01-dependent lysis of DIPG cells that express physiological levels of H3.3K27M. To demonstrate that the reactivity of TCR-transduced T cells is specific to H3.3K27M, we used HLA-A*02:01$^+$H3.3K27M^{neg} U87MG glioma cells that were stably transduced with cDNA encoding H3.3K27M (U87H3.3K27M) or H3.3WT (U87H3.3WT; Fig. 6, E and F). TCR-transduced T cells efficiently lysed U87H3.3K27M cells but not U87H3.3WT cells. Lysis of U87H3.3K27M cells was enhanced when synthetic H3.3K27M peptide was added but abrogated by the anti–HLA-A2 blocking antibody. On the other hand, TCR-transduced T cells lysed U87H3.3WT cells only when loaded with synthetic H3.3K27M peptide (Fig. 6 E). As an additional method to confirm the H3.3K27M and HLA-A*02:01 specific cytotoxicity of TCR-transduced T cells, we used carboxyfluorescein succinimidyl ester (CFSE)-stained target cells (U87H3.3K27M and U87H3.3WT) in the co-culture assay and evaluated the expression of 7-aminoactinomycin D (7-AAD) on the CFSE$^+$ target cells as an early marker for cell death (Lecoeur et al., 2001; Fig. 6 F). Our results confirmed those obtained by LDH-based assay. These results indicate that TCR-transduced T cells are able to recognize the H3.3K27M epitope that is processed and presented by H3.3K27M$^+$HLA-A*02:01$^+$ glioma cells and specifically lyse those glioma cells.

TCR-transduced T cells significantly inhibit progression of H3.3K27M$^+$ glioma xenograft

To determine the preclinical therapeutic activities of TCR-transduced T cells in vivo, we injected 5×10^4 U87H3.3K27M luciferase$^+$ cells into the brains of immu-

nocompromised NSG mice on day 0. On days 14 and 30, mice with established tumors received intravenous injections of either PBS, 5×10^6 control mock-transduced T cells, or 5×10^6 TCR-transduced T cells. Bioluminescence imaging (BLI) indicated a significant reduction in the tumor burden in mice receiving TCR-transduced T cells but not in mice receiving PBS or mock-transduced T cells (Fig. 7, A and B). After day 31, regardless of the tumor size, mice receiving either mock-transduced or TCR-transduced T cells started to present signs suggestive of graft-versus-host disease, such as ruffled fur, hunched posture, slow mobility, and weight loss (not depicted), and thus we were unable to evaluate the impact of therapy on long-term survival. Nonetheless, in an attempt to determine the accumulation of TCR-transduced T cells in the intracranial xenograft, we killed the mice on day 32 (2 d after T cell infusion) and evaluated tumor-infiltrating lymphocytes using the HLA-A*02:01-H3.3K27M$_{26–35}$ dextramer as well as anti-CD8 and anti-CD4 monoclonal antibodies. Although the transduction efficiency of the infused CD8$^+$ and CD4$^+$ cells was ~50% and 30%, respectively (Fig. 7 C), we found that >80% and 40% of human CD8$^+$ and CD4$^+$ T cells, respectively, were positive for the dextramer in the tumor. On the other hand, ~10% and 20% of CD8$^+$ and CD4$^+$ T cells were dextramer positive in the peripheral blood (Fig. 7 C). These data suggest that there was a selective accumulation of TCR-transduced T cells in the intracranial tumor site 2 d after T cell infusion. Our evaluation on the presence and function of infused T cells at longer time points was challenged by the regression of the tumor and associated disappearance of T cells from the brain (Fig. S1). Nonetheless, we observed TCR-transduced CD4$^+$ and CD8$^+$ cells in the spleen, lung, and peripheral blood 10 d after infusion. Further studies are warranted using syngeneic models to evaluate the precise interactions between TCR-transduced T cells and the host environment.

DISCUSSION

In the current study, we identified a novel HLA-A*02:01-restricted neoantigen epitope encompassing the H3.3K27M mutation, which is present in the majority of DMG in children and young adults (Solomon et al., 2016; Chiang and Ellison, 2017). Furthermore, we cloned a high-affinity TCR that specifically recognizes the H3.3K27M epitope endogenously expressed by H3.3K27M$^+$HLA-A*0201$^+$ glioma cells.

Heteroclitic peptide modifications to tumor antigen T cell epitopes have been described in the literature. Especially, replacement of the amino acid residue at position 2 to methionine has increased binding to HLA-A*02:01 and CTL-inducing ability of gp100$_{209–217}$ epitope (Dionne et al., 2003; Rosenberg et al., 2005). It is interesting that the H3.3K27M hotspot mutation has a fortuitous substitution of methionine at position 27 (position 2 of the epitope peptide)

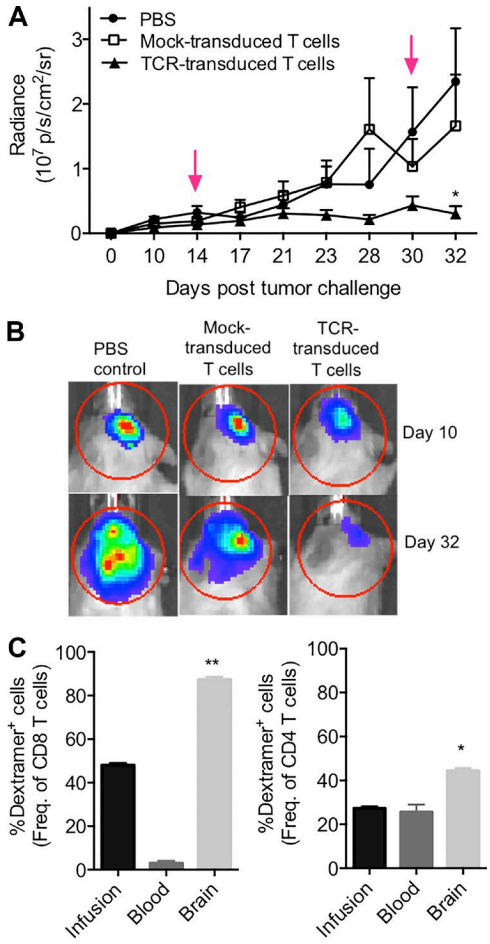

Figure 7. **Adoptive transfer of TCR-transduced T cells but not mock-transduced T cells results in inhibition of intracranial H3.3K27M$^+$ glioma in NSG mice.** NSG mice bearing intracranial U87H3.3K27M luciferase$^+$ gliomas received intravenous infusion with PBS, mock-transduced T cells or TCR-transduced T cells. **(A)** Tumor growth is presented as radiance (10^7 p/s/cm^2/r) using BLI. Arrows indicate days on which mice received treatment. Lines and error bars represent median and SD, respectively, for radiance (10^7 p/s/cm^2/r) using BLI (n = 8 per group). **(B)** Representative BLI images of mice on days 10 and 32 after tumor inoculation. The background BLI signals were defined based on the levels seen in non–tumor-bearing mice. **(C)** Preferential accumulation of TCR$^+$ T cells in the tumor site. At the time of intravenous infusion, ~50% and 30% of the infused CD8$^+$ and CD4$^+$ T cells, respectively, were dextramer$^+$ for TCR. On day 2 after the second intravenous infusion, the percentage of dextramer$^+$ cells among CD8$^+$ T cells and CD4$^+$ T cells was evaluated in the peripheral blood and brain of mice that received TCR-transduced T cells. Bars and error bars represent median and SD, respectively, for percentage of dextramer$^+$ cells among total live CD8$^+$ or CD4$^+$ T cells. Data indicate percentage dextramer$^+$ cells among total live CD8$^+$ or CD4$^+$ T cells (n = 5 per group). The experimental results shown in this figure are representative of two independent experiments with reproducible results. *, $P < 0.05$; **, $P < 0.01$ using Student's t test.

that naturally generates a heteroclitic peptide with improved HLA-A2 binding and immunogenicity compared with the nonmutated H3.3WT peptide.

Although most missense mutation–derived neoantigens are unique to individual patients (Tran et al., 2015, 2016), we expect that immunotherapy targeting the H3.3K27M epitope could be applicable to hundreds of patients annually in the United States and elsewhere, based on the high frequency of the H3.3K27M mutation and prevalence of HLA-A*02:01 (http://www.cbtrus.org; Zhang et al., 2017). We were able to detect H3.3K27M-specific T cell responses in DIPG patient–derived PBMCs but not healthy donor–derived PBMCs. Although these observations may imply that spontaneous H3.3K27M-specific T cell responses are not sufficient to control the tumor growth, these observations also substantiate our MS analysis demonstrating the presence of the H3.3K27M epitope in the HLA class I of H3.3K27M$^+$ glioma cells. During the submission and revision processes of the current article, Ochs et al. (2017) reported that a peptide encompassing the H3.3K27M induces specific CTL and Th1 responses in HLA-A2.DR1 transgenic mice. Although their study did not identify antigen-specific CTL clones or TCR cDNA, it confirms our results regarding the immunogenicity of the H3.3K27M epitope in HLA-A2$^+$ hosts. Together, these findings provide a rationale for enhancing the response by the peptide vaccine. In fact, we recently implemented a multicenter pilot study to evaluate the safety, immunoreactivity, and preliminary efficacy of a vaccine using the synthetic H3.3K27M$_{26–35}$ epitope peptide in children with H3.3K27M$^+$ DIPG or high-grade glioma through the Pacific Pediatric Neuro-Oncology Consortium (PNOC-007; NCT02960230).

Although the list of antigens that could be used for glioma immunotherapy has expanded over the last decade (Okada et al., 2009; Reardon et al., 2013), including those identified (Okano et al., 2002; Eguchi et al., 2006) or characterized (Hatano et al., 2005; Zhang et al., 2007) by our group, there have not been many truly glioma-specific antigens, except for those derived from EGFRvIII (Ohno et al., 2013; Johnson et al., 2015) and IDH1 (Schumacher et al., 2014). Furthermore, because of the marked heterogeneity of genetics and protein expression in solid cancers, targeting a single antigen may result in the evolution of tumor variants that lack the target antigen (Genßler et al., 2015; Navai and Ahmed, 2016). These observations underscore the need for expanding the list of available tumor-specific antigens, such as mutation-derived antigens (i.e., neoantigens), for safe and effective immunotherapy. The H3.3K27M-derived neoantigen epitope will be a valuable target because not only is it tumor specific, but the K27M mutant protein is also present throughout all tumor nuclei in each of the 47 cases evaluated by immunohistochemistry (Solomon et al., 2016), suggesting that this may be a truncal mutation and less likely to lead to antigen loss–mediated escape of the tumor. Given the recent occurrence of life-threatening and fatal events in cancer immunotherapy trials caused by on-target (Johnson et al., 2009; Morgan et al., 2010; Parkhurst et al., 2011) or off-target (Cameron et al., 2013; Morgan et al., 2013) cross-reactivity of T cells against normal cells, we focused our attention on addressing the antigen specificity of the TCR by performing alanine scanning (Cunningham and Wells, 1989; García-Peydró et al., 2000; Cameron et al., 2013).

Although our results revealed the absence of any known human proteins that share the same amino acid motif for recognition by the TCR, we also recognize that alanine scanning may not exclude all possibilities of cross-reactivity. In fact, although it was not at statistically significant levels, we observed a trend that TCR-transduced CD8$^+$ T cells produced modest numbers of IFN-γ spots against T2 cells loaded with a supraphysiological (10 μg/ml) concentration of H3.3WT peptide, suggesting a theoretical possibility of off-tumor reactivity. A full scan using a panel of all possible amino acid substitution combinations across the epitope would allow the derivation of a full pattern, or motif, for every potentially tolerated peptide and would provide the most comprehensive information.

Nonetheless, our data from the alanine scan provide us with a basis for understanding peptide specificity and how to evade potential cross-reactivity–induced toxicities. To further elucidate the specificity and cross-reactivity of the TCR, we have initiated a collaborative effort by integrating structural biology to characterize the interaction between the TCR and peptide-loaded HLA complexes (Adams et al., 2016).

The amino acid sequence of the A6 peptide in the alanine scan assay is identical to the peptide encompassing residues 26–35 of the H3.1 sequence and including the K27M mutation (Wu et al., 2012). The diminished peptide-HLA-A*02:01 binding and TCR recognition with the A6 peptide strongly suggests that our TCR will not be applicable to patients with the H3.1K27M mutation. Similarly, based on our alanine scanning data, if the tumor bears citrullinated R26 in addition to the K27M mutation in H3.3, the TCR will not likely respond. Hence, future clinical trials may need to evaluate patients' glioma tissue for citrullination of R26 in H3.3 as a part of eligibility screening, if a feasible evaluation method becomes available. Furthermore, our peptide binding assays with HLA-A2 subtypes suggested that the H3.3K27M epitope peptide may not bind efficiently to HLA-A2 subtypes other than HLA-A*02:01. This has to be considered in our considerations of patient eligibility.

Our SPR data indicated that the affinity of the TCR to H3.3K27M-HLA-A*02:01 is comparable to that of well-characterized high-affinity TCRs specific for viral or bacterial antigens (Aleksic et al., 2012). Nonviral cancer or self-antigen peptides usually bind TCRs at lower affinity levels (K_D 50–200 μM), as high-affinity TCRs to self-antigens are likely to be negatively selected in thymus. Although the kinetics of the TCR-H3.3K27M-HLA-A2 interaction was too fast to be accurately determined by our SPR experiment, fast kinetics is a salient feature for TCR-peptide HLA class I interactions (Cole et al., 2007).

Based on our peptide titration assay using primary human $CD8^+$ T cells transduced with the TCR, the EC_{50} ranges from 10^{-8} to 10^{-9} M, which is at least comparable with several known HLA-binding epitopes derived from melanoma antigens (Bakker et al., 1995; Lupetti et al., 1998). On the other hand, TCR-transduced $CD4^+$ T cells failed to demonstrate comparable responses, strongly suggesting the requirement of CD8 coreceptor for sufficient functions of the TCR. These data also imply a benefit of selecting $CD8^+$ T cells for transduction of the TCR in future clinical trials.

With regard to the TCR transduction system, a widely described pitfall in the use of TCR transduced T cells is mispairing between endogenous and transgene-derived α and β TCR chains, leading to reduced transgene TCR expression, unanticipated off-target reactivity, and/or autoimmunity (Govers et al., 2010; Zhang and Morgan, 2012). To ensure and enhance proper pairing of transgene-derived α and β-chains, a variety of gene-engineering technologies have been evaluated, such as introduction of a disulfide bridge in the α/β constant regions by the addition of extra cysteine residues, substituting human with murine constant regions, codon optimization, TCR chain leucine zipper fusions, and a single-chain TCR (Govers et al., 2010; Zhang and Morgan, 2012). In the current study, we were able to achieve excellent expression of the transgene TCR chains by incorporation of siRNA against the endogenous TCR (Okamoto et al., 2009, 2012) and cDNA codon optimization.

Our data from the MS analysis of U87H3.3K27M cells and cytotoxic assays using HSJD-DIPG-017 cells indicate that the H3.3K27M epitope is naturally produced and presented by HLA-A*02:01 on the surface of $H3.3K27M^+$ glioma cells. Our MS analysis as well as in vivo xenograft studies used U87H3.3K27M cells but not bona fide DIPG cells, such as HSJD-DIPG-017. This was because both assays require large numbers of cells (e.g., 5×10^8 cells needed for a single round of MS analysis), and none of bona fide DIPG cell lines could be grown in sufficient quantities within a reasonable time frame. Nevertheless, our datasets using a variety of cell lines support our important conclusion that the H3.3K27M epitope in glioma cells is targetable by the TCR.

Although our data with a xenograft model in NSG mice clearly demonstrated the efficacy of intravenously infused TCR-transduced T cells in vivo, we had limited opportunities to investigate precise interactions between the infused T cells and the host environment in immunocompromised mice. We have addressed our major focus on molecular factors, such as a chemokine, CXCL10 (Zhu et al., 2010; Ohkuri et al., 2014), and an integrin receptor, very late activation antigen (VLA)-4, which promote T cell infiltration in brain tumors using syngeneic models (Sasaki et al., 2007; Zhu et al., 2007). We will need to integrate these findings into the development of effective TCR-transduced T cell therapy approaches.

Data from the current study provide a solid foundation to develop safe and effective T cell–based immunotherapy targeting the H3.3K27M epitope. Recent studies have suggested that robust antitumor immune responses might be achieved by adoptive transfer of ex vivo–activated T cells (Rosenberg and Restifo, 2015). Therefore, we will direct our translational efforts to further optimize our TCR and develop effective T cell adoptive therapy for patients with $H3.3K27M^+$ gliomas.

MATERIALS AND METHODS

Cells and cell culture

DIPG neurosphere cultures were maintained in tumor stem medium containing Neurobasal-A Medium (1×), DMEM/F-12, Hepes buffer, sodium pyruvate, MEM nonessential amino acids, GlutaMAX-I, anti-anti solution, and B-27 supplement minus vitamin A or Gem21 neuroplex, all purchased from Life Technologies. Medium was supplemented with 20 ng/ml recombinant human EGF (rhEGF; AF-100-15; Peprotech), 20 ng/ml rhFGF-basic (AF-100-18B; Peprotech), 10 ng/ml hPDGF-AA (100-13A; Peprotech), 10 ng/ml hPDGF-BB (100-14B; Peprotech), and 2 µg/ml heparin solution (H3149-10KU; Sigma-Aldrich) at initiation of cell culture and weekly thereafter. Cells were passaged by trituration in TrypLE Express (12604-039; Invitrogen) and DNase1 (LS002007; Worthington) followed by resuspension in fresh medium. U87H3.3K27M and U87H3.3WT were generated by transfection of a PT2/C vector encoding cDNA for either WT H3.3 or the K27M H3.3 into parental $HLA\text{-}A2^*01^+$ $H3.3K27M^{neg}$ U87MG cells using FuGENE HD transfection reagent (E2311; Promega). Expression of H3.3K27M was confirmed by Western blot analysis with an anti-H3.3K27M antibody (ABE419; Millipore). HSJD-DIPG019 cells were transduced with lentiviral vector encoding *HLA-A2*01* cDNA with puromycin selection marker (VectorBuilder) for generation of HSJD-DIPG019-HLA-A2*01 cells. The Jurkat T cell clone 76 (J76CD8) cell line (Heemskerk et al., 2003), which is deficient in endogenous TCR α- and β-chains but express human CD8, was provided by M. Heemskerk (Leiden University Medical Center, Leiden, Netherlands). Cell lines used were confirmed to be negative for mycoplasma infection.

T cell isolation

LRS chambers containing healthy donor–derived HLA-A*02:01$^+$ PBMCs were obtained from the Stanford Blood Bank. Patient-derived PBMCs were obtained through the Institutional Review Board–approved Neurosurgery Tissue Bank (IRB/CHR# 10-01318; PI, J. Phillips) with coded tissue information without any protected health identifiers. T cells were enriched from whole blood by immunodensity isolation using the RosetteSep Human T cell Enrichment Cocktail (15061; Stem Cell Technologies) according to the manufacturer's suggested protocol. T cells were cryopreserved in RPMI medium containing 20% human AB serum and 10% DMSO and stored at −196°C.

Peptides

The synthetic peptides $H3.3K27M_{26–35}$ (RMSAPSTGGV), $H3.3WT_{26–35}$ (RKSAPSTGGV), $CITmH3.3_{26–35}$ (XMSAPS

TGGV), H3.1K27M$_{26–35}$ (RMSAPATGGV), and influenza matrix protein M1$_{58–66}$ flu peptide (GILGFVFTL), as well as peptides used for the alanine scanning assay, were synthesized by A&A Laboratories and were >95% pure as indicated by analytic HPLC and MS analyses. Peptides were dissolved in DMSO at a concentration of 10 mg/ml and stored at −80°C until use.

HLA–peptide binding assays

Quantitative assays to measure the binding of peptides to purified HLA A*02:01 class I molecules are based on the inhibition of binding of a radiolabeled standard peptide (HBV core 18–27 analogue, FLPSDYFPSV) and were performed as detailed elsewhere (Sidney et al., 2013). HLA molecules were purified by affinity chromatography from the EBV-transformed homozygous cell line JY, as described previously (Sidney et al., 2013). Peptides were tested at six different concentrations covering a 100,000-fold dose range in three or more independent assays, and the IC_{50} of the binding of the radiolabeled probe peptide was calculated. Under the conditions used, where [radiolabeled probe] < [MHC] and $IC_{50} \geq$ [MHC], the measured IC_{50} values are reasonable approximations of the true K_D values (Cheng and Prusoff, 1973; Gulukota et al., 1997).

ELISPOT assays

Patient-derived and healthy donor–derived PBMCs were stimulated with 10 µg/ml H3.3K27M$_{26–35}$ peptide or H3.3WT$_{26–35}$ peptide, or flu peptide or without peptide. At 48 h, rhIL-2 (50 U/ml), IL-7 (10 ng/ml), and IL-15 (10 ng/ml) were added to the culture for an additional 5 d. 5×10^4 peptide-stimulated T cells were co-cultured with 5×10^4 T2 cells pulsed with 10 µg/ml H3.3K27M$_{26–35}$ peptide or H3.3WT$_{26–35}$ peptide or without peptide for 24 h on ELISPOT plates coated with anti–human IFN-γ antibody. To determine TCR avidity, 5×10^4 TCR-transduced CD8$^+$ T cells were co-cultured with 5×10^4 T2 cells pulsed with different concentrations of the H3.3K27M peptide overnight on ELISPOT plates coated with anti–human IFN-γ antibody. The rest of the protocol was performed according to the manufacturer's protocol (human IFN-γ ELISPOT kit; 552138; BD). The spots were quantified using the CTL S6 Universal-V Analyzer ELISpot Reader (ImmunoSpot).

Purification and LC-MS/MS analysis of HLA class I peptides

HLA class I complexes were purified from 5×10^8 U87 parental cells or U87 cells transfected with either H3.3WT or H3.3K27M, as previously described (Bassani-Sternberg et al., 2015). In brief, cells were lysed with 0.25% sodium deoxycholate (Sigma-Aldrich), 1% octyl-β-D-glucopyranoside (Sigma-Aldrich), 0.2 mM iodoacetamide, 1 mM EDTA, and 1:200 protease inhibitor cocktail (Sigma-Aldrich) in PBS at 4°C for 1 h. The lysate was cleared by 30-min centrifugation at 40,000 *g* at 4°C. HLA class I complexes were immunoaffinity-purified from the cleared lysate with protein A Sepharose beads (Invitrogen) covalently bound to the pan-HLA class I antibody W6/32 (purified from HB95 cells; ATCC) and eluted at room temperature with 0.1 N acetic acid. Eluted HLA-I complexes were then loaded on Sep-Pak tC18 cartridges (Waters Corporation), and HLA class I peptides were separated from the complexes by eluting them with 30% acetonitrile (ACN) in 0.1% TFA. Peptides were further purified using Silica C-18 column tips (Harvard Apparatus), eluted again with 30% ACN in 0.1% TFA, and concentrated by vacuum centrifugation. For LC-MS/MS analysis, HLA class I peptides were separated on an EASY-nLC 1000 system (Thermo Fisher Scientific) coupled online to a Q Exactive HF mass spectrometer (Thermo Fisher Scientific) with a nanoelectrospray ion source (Thermo Fisher Scientific). Peptides were loaded in buffer A (0.1% formic acid) into a 50-cm-long, 75-µm-ID column in-house packed with ReproSil-Pur C18-AQ 1.9 µm resin (Dr. Maisch HPLC GmbH) and eluted with a 90-min linear gradient of 5–30% buffer B (80% ACN and 0.1% formic acid) at a 250 nl/min flow rate. The Q Executive HF operated in a data-dependent mode with full MS scans at the range of 300–1,650 m/z, with resolution of 60,000 at 200 m/z and a target value of 3×10^6 ions. The 10 most abundant ions with charge 1–3 were combined to give an AGC target value of 1×10^5 and a maximum injection time of 120 ms, fragmented by high-energy collisional dissociation (HCD). MS/MS scans were acquired with a resolution of 15,000 at 200 m/z, and dynamic exclusion was set to 20 s to avoid repeated peptide sequencing. Data were acquired and analyzed with the Xcalibur software (Thermo Fisher Scientific). For the targeted identification of the H3.3K27M peptide, a heavy (Arg10) version of the peptide was synthetized with the Fmoc solid phase method using the ResPepMicroScale instrument (Intavis AG Bioanalytical Instruments), introducing a 10.0083-D mass difference with one 13C6 15N4 arginine (AnaSpec). The heavy peptide was added to each sample at a 1-pmol/µl concentration for a total of 3 pmol per run.

For MS data analysis, raw files were processed using MaxQuant version 1.5.7.12 as described previously (Bassani-Sternberg et al., 2015). Searches were performed against the Human UniProt database (July 2015) and a customized reference database containing the H3.3K27M sequence. Enzyme specificity was set as unspecific, and possible sequence matches were restricted to 8–15 amino acids and a maximum mass of 1500 D. N-terminal acetylation and methionine oxidation were set as variable modifications. A false discovery rate of 0.01 was required at the peptide level. To identify the heavy peptide, an Arg10 label was added to the search type specification.

Induction and isolation of H3.3K27M-specific CTL clones

To generate dendritic cells, the plastic-adherent cells from PBMCs were cultured in AIM-V medium (Invitrogen) supplemented with 1,000 units/ml recombinant human GM-CSF and 500 units/ml rhIL-4 (Cell Sciences) at 37°C in

a humidified CO_2 (5%) incubator. 6 d later, the immature dendritic cells were stimulated with recombinant human TNF-α, IL-6, and IL-1β (10 ng/ml each). Mature dendritic cells were then harvested on day 8, resuspended in AIM-V medium at 10^6 cells/ml with peptide (10 μg/ml), and incubated for 2 h at 37°C. Populations of autologous $CD8^+$ T cells were enriched from PBMCs using magnetic microbeads (Miltenyi Biotec). $CD8^+$ T cells (2×10^6 per well) were co-cultured with 2×10^5/well peptide-pulsed dendritic cells in 2 ml/well AIM-V medium supplemented with 5% human AB serum, 10 U/ml rhIL-2 (R&D Systems), and 10 units/ml rhIL-7 (Cell Sciences) in each well of 24-well tissue culture plates. On day 15, lymphocytes were restimulated with autologous dendritic cells pulsed with peptide in AIM-V medium supplemented with 5% human AB serum, rhIL-2, and rhIL-7 (10 units/ml each).

HLA-A*0201–peptide tetramer staining

PE-conjugated HLA-A*0201 RMSAPSTGGV tetramer (H3.3K27M-tetramer) was produced by the National Institute of Allergy and Infectious Disease tetramer facility within the Emory University Vaccine Center (Atlanta, GA) using the peptide synthesized by A&A Laboratories. PE-conjugated HLA-A*0201/RMSAPSTGGV Dextramer was purchased from Immudex. Cells were stained with tetramer (10 μg/ml) or dextramer in PBS containing 1% BSA for 15 min at 4°C (for tetramer) or room temperature (for dextramer), followed by surface staining for various T cell markers at 4°C. Cells were then washed with PBS containing 0.1% BSA. For some experiments, T cells were stained with tetramer, followed by anti–human CD3 FITC (344803; BioLegend), CD4-PerCPCy.5.5 (317427; BioLegend), CD8 APC (344722; BioLegend), CD69 FITC (11-0699-42; eBioscience), or PD-1-PECy7 (561272; BD Biosciences) along with the suitable isotype control antibodies. Intracellular cytokine staining was performed using Fixation/Permeabilization Solution kit (54714; BD Biosciences) according to the manufacturer's instructions. T cells were then stained with anti–human Granzyme-B-BV421 (563389; BD Biosciences). The cells were acquired using a Sony SH800 flow cytometer and analyzed using FlowJo software v.10.

ELISA

Medium was collected and centrifuged at 500 *g* for 10 min to remove debris. Human IFN-γ (555142; BD OptEIA) and human IL-2 (EH2IL2; Thermo Fisher Scientific) ELISA was performed according to the manufacturers' protocol. Plates were analyzed on a Biotek Synergy2 microplate reader (Biotek) at wavelengths of 450 nm and a background of 550 nm.

Cloning of TCR

5′-Rapid amplification of cDNA ends (RACE)-PCR was performed by SMARTer RACE 5′/3′ kit (634838; Clontech). In brief, a single RACE-PCR product (~900 bp) was excised from a 1.2% agarose gel, purified by Zymoclean Gel DNA Recovery kit (Zymo; D4001), and TOPO cloned into Pcr-Blunt II-TOPO using the Zero Blunt TOPO PCR Cloning kit (K2800-20SC; Life Technologies). The cloned product was then transformed into MAX Efficiency DH5α Competent cells (182580120; Life Technologies) and plated on ampicillin-containing LB agar plates (L1004; Teknova). LB agar plates were placed at 37°C overnight to allow colonies to form. Selected clones from the resulting constructs were subjected to PCR amplification and sequencing (Quintara-Bio) using the M13 (−21) forward primer (5′-TGTAAA ACGACGGCCAGT-3′) and M13 reverse primer (5′-CAG GAAACAGCTATGAC-3′) for sequencing. Sequences were analyzed using SnapGene Viewer.

Generation of siTCR retroviral producer cell lines

The siTCR system has been previously described (Okamoto et al., 2009, 2012). In brief, codon-optimized *TCRA* and *TCRB* fragments were artificially synthesized and cloned into Takara's siTCR retroviral vector plasmid. The vector was constructed in the following sequence: murine stem cell virus (MSCV) 5′ LTR promoter driving the TCR as well as siRNA, siRNA cassette, TCRβ, Spacer + P2A peptide, followed by TCRα sequence. The siRNA sequences were designed to bind and silence the endogenous TCRα and TCRβ constant regions but were mismatched to the codon-optimized TCRα and TCRβ constant regions of the H3.3K27M TCR. PG13 packaging cells were plated at 3×10^4 cells per well of a six-well plate and incubated for 24 h. PG13 cells were transfected with siTCR retroviral vector in the presence of 8 μg/ml polybrene and incubated for 4 h at 37°C, 5% CO_2; this was repeated on the next day. The cells were further expanded, harvested as GaLV envelope pseudo-typed siTCR retroviral vector producer cells, and cryopreserved. For generation of retroviral particles, culture supernatant was collected from cells grown in complete DMEM supplemented with 5 mM sodium butyrate (156-54-7; Sigma-Aldrich) for 24 h.

Production of recombinant TCR

Matured H3.3K27M TCR α and β ectodomains with an engineered C-domain interchain disulfide bond were separately cloned into the pAcGP67a insect expression vector (554756; BD Biosciences) encoding either a C-terminal acidic zipper-biotin acceptor peptide-6xHis tag or a C-terminal basic zipper-6xHis tag. A 3c protease site was introduced between the C-terminal TCR (α or β) ectodomain and (acidic or basic) zipper sequence (Birnbaum et al., 2014). Baculoviruses for each TCR construct were produced in SF9 cells. TCR production was performed in High Five cells by transfecting with appropriate ratio of TCRα and TCRβ viruses for 48–72 h at 30°C. Harvested culture medium was incubated with Ni-NTA resin (30250; Qiagen) at room temperature for 3 h and eluted in 1× Hepes-buffered saline (HBS) + 200 mM imidazole (pH 7.2). Eluted TCR was buffer-exchanged to 1× HBS and incubate with the appropriate amount of 3 C protease (100 ng/μl) at 4°C overnight. The reaction was then

purified via size-exclusion chromatography using an AKT APurifier (GE Healthcare) on a Superdex 200 column (GE Healthcare). Peak fractions were pooled and run on SDS-PAGE gel as quality controls.

Soluble HLA-A2 loaded with H3.3K27M peptide (RMSAPSTGGV) was prepared by in vitro folding. The HLA-A2 heavy chain (residues 1–275) and β2 microglobulin (residues 1–100) were separately cloned into pET-26b vector and transformed by Rosseta DE3 *Escherichia coli* cells. Inclusion bodies containing corresponding proteins were dissolved in 8 M urea, 50 mM Tris-HCl, pH 8.0, 10 mM EDTA, and 10 mM DTT. For in vitro folding, the HLA-A2 heavy chain, β2-microglobulin, and H3.3K27M peptide were mixed in a 1:2:10 molar ratio and diluted into a folding buffer containing 0.4 M L-arginine-HCl, 100 mM Tris-HCl, pH 8.0, 5 mM EDTA, 0.5 mM oxidized glutathione, and 5 mM reduced glutathione (Garboczi et al., 1992). After 72 h at 4°C to dialyze against 10 liters of 10 mM Tris-HCl, the folding mixture was subjected on a weak ion exchange column (DEAE cellulose). Folded H3.3K27M-HLA-A2 was purified using sequential size exclusion chromatography (Superdex 200 column) and ion-exchange chromatography (Mono Q columns).

SPR analysis

The interaction of the TCR with H3.3K27M peptide-HLA-A2 was measured by SPR using a BIAcore T100 biosensor at 25°C. Biotinylated H3.3K27M-HLA-A2 was immobilized on a streptavidin-coated BIAcore SA chip (GE Healthcare) at 300 resonance units (RU). A different flow cell was immobilized with nonrelevant peptide-HLA-A2 to serve as blank control. Different concentrations 1H5 TCR solution were flowed sequentially over blank and H3.3K27M-HLA-A2. Injections of TCR were stopped 60 s after start of injections to allow sufficient time for SPR signals to reach plateau. Dissociation constants (K_D) were obtained by fitting equilibrium data with a 1:1 binding model using BIAcore evaluation software.

Infection of primary T cells with TCR vector

Human PBMCs were activated on plates precoated with anti–human CD3 antibody (OKT3 clone; 170-076-124; Miltenyi Biotec) and RetroNectin (T100A; Takara Bio). 3 d after the stimulation, viral supernatant (for TCR-transduction groups) or PBS (for mock-transduction groups) was spun on separate RetroNectin-coated plates at 2,000 *g* for 2 h at 4°C. Activated PBMCs were harvested from the OKT3-RetroNectin plates and added to the virus-coated plates using spinfection methodology at 1,000 *g* for 10 min at 4°C, and the cells were supplemented with 600 U/ml IL-2 (200-02; PeproTech). This transduction protocol was repeated on the next day, and PBMCs were allowed to rest for an additional 4 d and then were stained with HLA-A*02:01-H3.3K27M tetramer to determine the transduction efficiency. The T cells were maintained in 100 U/ml rhIL-2-containing freshly made GT-T551 medium (WK551S; Takara Bio).

LDH-based cytotoxicity assay

The CytoTox 96 nonradioactive cytotoxicity assay (Promega) was performed according to the manufacturer's protocol. Target cells were plated in 96-well plates with various effector/target (E/T) ratios in 200 µl media for 24 h. 50 µl supernatant was then transferred to an enzymatic assay plate containing 50 µl CytoTox 96 Reagent and incubated for 30 min at room temperature. Stop solution was then added to each well, and plates were analyzed at 490 nm on a Synergy2 microplate reader (Biotek). Percentage cytotoxicity was calculated as [(experimental − effector spontaneous − target spontaneous)/(target maximum − target spontaneous)] × 100.

CSFE-based cytotoxicity assay

Target cells were stained with CFSE using the Vybrant CFDA SE Cell Tracer kit (V12883; Thermo Fisher Scientific). CFSE-labeled target cells (5×10^4/well) were incubated with CTLs at the E/T ratio of 5 for 8 h. To block HLA-A2–mediated lysis, anti-HLA-A2 antibody (10 µg/ml; 343302; BioLegend) was added to one group per experiment. At the end of incubation, 7-AAD (420403; BioLegend) was added into each well and incubated for 10 min on ice. The samples were analyzed by flow cytometry, and the killed target cells were identified as $CFSE^+7\text{-}AAD^+$ cells. Cytotoxicity was calculated as the percentage of $CFSE^+$ and $7\text{-}AAD^+$ cells in total $CFSE^+$ cells.

Therapy of mice bearing intracranial glioma xenografts

5–6-wk-old NOD.Cg-*Prkdc*^{scid}*Il2rg*^{tm1Wjl}/SzJ (NSG mice) female mice (Jackson Laboratory) were used in the experiments. Animals were handled in the Animal Facility at the University of California, San Francisco (UCSF), per an Institutional Animal Care and Use Committee (IACUC)-approved protocol. The procedure has been previously described by us (Ohno et al., 2013). In brief, using a stereotactic apparatus, mice received 5×10^4 U87H3.3K27M luciferase-expressing cells/mouse in 2 µl PBS at 2 mm lateral to the bregma and 3 mm below the surface of the skull. After tumors were established, each mouse received intravenous infusions of PBS, mock-transduced T cells, or 5×10^6 TCR-transduced T cells via the tail vein on days 14 and 30 after tumor inoculation. In some experiments, mice were killed at 2 or 10 d after T cell transfusion. Spleen, blood, lung, and tumors were harvested and enumerated for CD8, CD4, tetramer, granzyme-B, and PD-1.

Bioluminescence imaging

The growth of luciferase-positive U87H3.3K27M tumors in the brain was noninvasively monitored by BLI using the in vivo imaging system IVIS 100 (PerkinElmer). Mice received i.p. injections with 200 µl (15 mg/ml) of aqueous solution of D-luciferin potassium salt (PerkinElmer) and were anesthetized with isoflurane, then imaged for bioluminescence for 1 min of exposure time. The imaging of tumors was performed in a blinded fashion. Optical images were analyzed with the IVIS Living Image software package.

Statistical analyses

All statistical analyses were performed on GraphPad Prism v.6.0h software. For in vitro studies, Student's *t* test or one-way ANOVA was used to compare two groups or more than two groups, respectively. Nonlinear regression analysis was used to determine the EC_{50}. We considered differences significant when $P < 0.05$.

Study approval

All mouse studies were performed under a UCSF IAC UC–approved protocol. Clinical samples (PBMCs) were obtained from the Brain Tumor Research Center Tissue Core at UCSF under a protocol approved by the UCSF Committee on Human Research.

Online supplementary material

Fig. S1 shows the distribution of adoptively transferred TCR-transduced T cells in organs of NSG mice. Table S1 lists the binding affinity of H3.3K27M (26–35) mutant versus H3.3WT (26–35) nonmutant peptides to HLA-A2 subtypes. Table S2 lists human proteins with amino acid motifs that are homologous to the key amino acid residues recognized by the TCR. Table S3 lists HLA class I typing data of the cell lines used in the current study.

ACKNOWLEDGMENTS

We thank Dr. Michael Nishimura (Loyola University) for technical advice for transduction of human T cells with the TCR, Drs. Kazuto Takesako and Hideto Chono (Takara Bio Inc.) for preparation of the retroviral TCR vector, and the Preclinical Therapeutics Core at the University of California, San Francisco, for the use of the Xenogen Imaging System.

The current study was supported by NIH/National Institute of Neurological Disorders and Stroke (NINDS) R01NS096954 (H. Okada), NIH/NINDS 2R01NS055140 (H. Okada), the National Center for Advancing Translational Sciences, NIH, through University of California, San Francisco Clinical & Translational Science Institute (H. Okada), V Foundation for Cancer Research D2015-018 (S. Mueller and H. Okada), Parker Institute for Cancer Immunotherapy (H. Okada), NIH/National Cancer Institute 1T32CA151022 (G. Kohanbash), Fondo Alicia Pueyo CP13/00189 (A.M. Carcaboso), and Instituto de Salud Carlos III-Fondo Europeo de Desarrollo Regional PI15/01161 (A.M. Carcaboso).

H. Okada and Y. Hou are inventors of US utility patent application "H3.3 CTL peptides and uses thereof" (case SF2015-163). The authors declare no further competing financial interests.

Author contributions: I.F. Pollack, Y. Hou, and H. Okada conceived the study; Z.S. Chheda, G. Kohanbash, K.C. Garcia, Y. Hou, and H. Okada designed research studies; Z.S. Chheda, G. Kohanbash, K. Okada, N. Jahan, J. Sidney, X. Yang, D.A. Carrera, K.M. Downey, S. Shrivastav, S. Liu, Y. Lin, C. Lagisetti, P. Chuntova, and P.B. Watchmaker conducted experiments; Z.S. Chheda, G. Kohanbash, J. Sidney, S. Mueller, R. Rajalingam, A.M. Carcaboso, A. Sette, K.C. Garcia, Y. Hou, and H. Okada analyzed data; M. Pecoraro and M. Mann conducted mass spectrometry experiments; S. Mueller contributed to acquisition of patient-derived blood samples and provided insights from her clinical experience treating patients with DIPG; Z.S. Chheda, G. Kohanbash, J. Sidney, X. Yang, and H. Okada wrote the manuscript; and all authors contributed to reviewing and proofing of the manuscript.

Submitted: 8 June 2017
Revised: 1 October 2017
Accepted: 23 October 2017

REFERENCES

Adams, J.J., S. Narayanan, M.E. Birnbaum, S.S. Sidhu, S.J. Blevins, M.H. Gee, L.V. Sibener, B.M. Baker, D.M. Kranz, and K.C. Garcia. 2016. Structural interplay between germline interactions and adaptive recognition determines the bandwidth of TCR-peptide-MHC cross-reactivity. *Nat. Immunol.* 17:87–94. https://doi.org/10.1038/ni.3310

Aleksic, M., N. Liddy, P.E. Molloy, N. Pumphrey, A. Vuidepot, K.M. Chang, and B.K. Jakobsen. 2012. Different affinity windows for virus and cancer-specific T-cell receptors: Implications for therapeutic strategies. *Eur. J. Immunol.* 42:3174–3179. https://doi.org/10.1002/eji.201242606

Bakker, A.B., G. Marland, A.J. de Boer, R.J. Huijbens, E.H. Danen, G.J. Adema, and C.G. Figdor. 1995. Generation of antimelanoma cytotoxic T lymphocytes from healthy donors after presentation of melanoma-associated antigen-derived epitopes by dendritic cells in vitro. *Cancer Res.* 55:5330–5334.

Bassani-Sternberg, M., S. Pletscher-Frankild, L.J. Jensen, and M. Mann. 2015. Mass spectrometry of human leukocyte antigen class I peptidomes reveals strong effects of protein abundance and turnover on antigen presentation. *Mol. Cell. Proteomics.* 14:658–673. https://doi.org/10.1074/mcp.M114.042812

Birnbaum, M.E., J.L. Mendoza, D.K. Sethi, S. Dong, J. Glanville, J. Dobbins, E. Ozkan, M.M. Davis, K.W. Wucherpfennig, and K.C. Garcia. 2014. Deconstructing the peptide-MHC specificity of T cell recognition. *Cell.* 157:1073–1087. https://doi.org/10.1016/j.cell.2014.03.047

Brain Tumor Progress Review Group. 2000. Report of the Brain Tumor Progress Review Group. National Cancer Institute, National Institute of Neurological Disorders and Stroke, Bethesda, MD. NIH pub. no. 01-4902. Available at: https://permanent.access.gpo.gov/lps88132/2000braintumor.pdf

Cameron, B.J., A.B. Gerry, J. Dukes, J.V. Harper, V. Kannan, F.C. Bianchi, F. Grand, J.E. Brewer, M. Gupta, G. Plesa, et al. 2013. Identification of a Titin-derived HLA-A1-presented peptide as a cross-reactive target for engineered MAGE A3-directed T cells. *Sci. Transl. Med.* 5:197ra103. https://doi.org/10.1126/scitranslmed.3006034

Cheng, Y., and W.H. Prusoff. 1973. Relationship between the inhibition constant (K1) and the concentration of inhibitor which causes 50 per cent inhibition (I50) of an enzymatic reaction. *Biochem. Pharmacol.* 22:3099–3108. https://doi.org/10.1016/0006-2952(73)90196-2

Chiang, J.C., and D.W. Ellison. 2017. Molecular pathology of paediatric central nervous system tumours. *J. Pathol.* 241:159–172. https://doi.org/10.1002/path.4813

Cole, D.K., N.J. Pumphrey, J.M. Boulter, M. Sami, J.I. Bell, E. Gostick, D.A. Price, G.F. Gao, A.K. Sewell, and B.K. Jakobsen. 2007. Human TCR-binding affinity is governed by MHC class restriction. *J. Immunol.* 178:5727–5734. https://doi.org/10.4049/jimmunol.178.9.5727

Cunningham, B.C., and J.A. Wells. 1989. High-resolution epitope mapping of hGH-receptor interactions by alanine-scanning mutagenesis. *Science.* 244:1081–1085. https://doi.org/10.1126/science.2471267

Cuthbert, G.L., S. Daujat, A.W. Snowden, H. Erdjument-Bromage, T. Hagiwara, M. Yamada, R. Schneider, P.D. Gregory, P. Tempst, A.J. Bannister, and T. Kouzarides. 2004. Histone deimination antagonizes arginine methylation. *Cell.* 118:545–553. https://doi.org/10.1016/j.cell.2004.08.020

Dionne, S.O., M.H. Smith, F.M. Marincola, and D.F. Lake. 2003. Functional characterization of CTL against gp100 altered peptide ligands. *Cancer Immunol. Immunother.* 52:199–206.

Eguchi, J., M. Hatano, F. Nishimura, X. Zhu, J.E. Dusak, H. Sato, I.F. Pollack, W.J. Storkus, and H. Okada. 2006. Identification of interleukin-13 receptor alpha2 peptide analogues capable of inducing improved antiglioma CTL responses. *Cancer Res.* 66:5883–5891. https://doi.org/10.1158/0008-5472.CAN-06-0363

Garboczi, D.N., D.T. Hung, and D.C. Wiley. 1992. HLA-A2-peptide complexes: Refolding and crystallization of molecules expressed in

Escherichia coli and complexed with single antigenic peptides. *Proc. Natl. Acad. Sci. USA.* 89:3429–3433. https://doi.org/10.1073/pnas.89.8.3429

García-Peydró, M., A. Paradela, J.P. Albar, and J.A. Castro. 2000. Antagonism of direct alloreactivity of an HLA-B27-specific CTL clone by altered peptide ligands of its natural epitope. *J. Immunol.* 165:5680–5685. https://doi.org/10.4049/jimmunol.165.10.5680

Genßler, S., M.C. Burger, C. Zhang, S. Oelsner, I. Mildenberger, M. Wagner, J.P. Steinbach, and W.S. Wels. 2015. Dual targeting of glioblastoma with chimeric antigen receptor-engineered natural killer cells overcomes heterogeneity of target antigen expression and enhances antitumor activity and survival. *OncoImmunology.* 5:e1119354. https://doi.org/10.1080/2162402X.2015.1119354

Govers, C., Z. Sebestyén, M. Coccoris, R.A. Willemsen, and R. Debets. 2010. T cell receptor gene therapy: Strategies for optimizing transgenic TCR pairing. *Trends Mol. Med.* 16:77–87. https://doi.org/10.1016/j.molmed.2009.12.004

Gulukota, K., J. Sidney, A. Sette, and C. DeLisi. 1997. Two complementary methods for predicting peptides binding major histocompatibility complex molecules. *J. Mol. Biol.* 267:1258–1267. https://doi.org/10.1006/jmbi.1997.0937

Hatano, M., J. Eguchi, T. Tatsumi, N. Kuwashima, J.E. Dusak, M.S. Kinch, I.F. Pollack, R.L. Hamilton, W.J. Storkus, and H. Okada. 2005. EphA2 as a glioma-associated antigen: A novel target for glioma vaccines. *Neoplasia.* 7:717–722. https://doi.org/10.1593/neo.05277

Heemskerk, M.H., M. Hoogeboom, R.A. de Paus, M.G. Kester, M.A. van der Hoorn, E. Goulmy, R. Willemze, and J.H. Falkenburg. 2003. Redirection of antileukemic reactivity of peripheral T lymphocytes using gene transfer of minor histocompatibility antigen HA-2-specific T-cell receptor complexes expressing a conserved alpha joining region. *Blood.* 102:3530–3540. https://doi.org/10.1182/blood-2003-05-1524

Johnson, L.A., R.A. Morgan, M.E. Dudley, L. Cassard, J.C. Yang, M.S. Hughes, U.S. Kammula, R.E. Royal, R.M. Sherry, J.R. Wunderlich, et al. 2009. Gene therapy with human and mouse T-cell receptors mediates cancer regression and targets normal tissues expressing cognate antigen. *Blood.* 114:535–546. https://doi.org/10.1182/blood-2009-03-211714

Johnson, L.A., J. Scholler, T. Ohkuri, A. Kosaka, P.R. Patel, S.E. McGettigan, A.K. Nace, T. Dentchev, P. Thekkat, A. Loew, et al. 2015. Rational development and characterization of humanized anti-EGFR variant III chimeric antigen receptor T cells for glioblastoma. *Sci. Transl. Med.* 7:275ra22. https://doi.org/10.1126/scitranslmed.aaa4963

Jones, C., and S.J. Baker. 2014. Unique genetic and epigenetic mechanisms driving paediatric diffuse high-grade glioma. *Nat. Rev. Cancer.* 14:651–661. https://doi.org/10.1038/nrc3811

Kebudi, R., and F.B. Cakir. 2013. Management of diffuse pontine gliomas in children: Recent developments. *Paediatr. Drugs.* 15:351–362. https://doi.org/10.1007/s40272-013-0033-5

Khuong-Quang, D.A., P. Buczkowicz, P. Rakopoulos, X.Y. Liu, A.M. Fontebasso, E. Bouffet, U. Bartels, S. Albrecht, J. Schwartzentruber, L. Letourneau, et al. 2012. K27M mutation in histone H3.3 defines clinically and biologically distinct subgroups of pediatric diffuse intrinsic pontine gliomas. *Acta Neuropathol.* 124:439–447. https://doi.org/10.1007/s00401-012-0998-0

Lagerwerf, F.M., M. van de Weert, W. Heerma, and J. Haverkamp. 1996. Identification of oxidized methionine in peptides. *Rapid Commun. Mass Spectrom.* 10:1905–1910. https://doi.org/10.1002/(SICI)1097-0231(199612)10:15<1905::AID-RCM755>3.0.CO;2-9

Lecoeur, H., M. Février, S. Garcia, Y. Rivière, and M.L. Gougeon. 2001. A novel flow cytometric assay for quantitation and multiparametric characterization of cell-mediated cytotoxicity. *J. Immunol. Methods.* 253:177–187. https://doi.org/10.1016/S0022-1759(01)00359-3

Louis, D.N., A. Perry, G. Reifenberger, A. von Deimling, D. Figarella-Branger, W.K. Cavenee, H. Ohgaki, O.D. Wiestler, P. Kleihues, and D.W. Ellison. 2016. The 2016 World Health Organization Classification of Tumors of the Central Nervous System: A summary. *Acta Neuropathol.* 131:803–820. https://doi.org/10.1007/s00401-016-1545-1

Lupetti, R., P. Pisarra, A. Verrecchia, C. Farina, G. Nicolini, A. Anichini, C. Bordignon, M. Sensi, G. Parmiani, and C. Traversari. 1998. Translation of a retained intron in tyrosinase-related protein (TRP) 2 mRNA generates a new cytotoxic T lymphocyte (CTL)-defined and shared human melanoma antigen not expressed in normal cells of the melanocytic lineage. *J. Exp. Med.* 188:1005–1016. https://doi.org/10.1084/jem.188.6.1005

Morgan, R.A., J.C. Yang, M. Kitano, M.E. Dudley, C.M. Laurencot, and S.A. Rosenberg. 2010. Case report of a serious adverse event following the administration of T cells transduced with a chimeric antigen receptor recognizing ERBB2. *Mol. Ther.* 18:843–851. https://doi.org/10.1038/mt.2010.24

Morgan, R.A., N. Chinnasamy, D. Abate-Daga, A. Gros, P.F. Robbins, Z. Zheng, M.E. Dudley, S.A. Feldman, J.C. Yang, R.M. Sherry, et al. 2013. Cancer regression and neurological toxicity following anti-MAGE-A3 TCR gene therapy. *J. Immunother.* 36:133–151. https://doi.org/10.1097/CJI.0b013e3182829903

Navai, S.A., and N. Ahmed. 2016. Targeting the tumour profile using broad spectrum chimaeric antigen receptor T-cells. *Biochem. Soc. Trans.* 44:391–396. https://doi.org/10.1042/BST20150266

Ochs, K., M. Ott, T. Bunse, F. Sahm, L. Bunse, K. Deumelandt, J.K. Sonner, M. Keil, A. von Deimling, W. Wick, and M. Platten. 2017. K27M-mutant histone-3 as a novel target for glioma immunotherapy. *OncoImmunology.* 6:e1328340. https://doi.org/10.1080/2162402X.2017.1328340

Ohkuri, T., A. Ghosh, A. Kosaka, J. Zhu, M. Ikeura, M. David, S.C. Watkins, S.N. Sarkar, and H. Okada. 2014. STING contributes to antiglioma immunity via triggering type I IFN signals in the tumor microenvironment. *Cancer Immunol. Res.* 2:1199–1208. https://doi.org/10.1158/2326-6066.CIR-14-0099

Ohno, M., T. Ohkuri, A. Kosaka, K. Tanahashi, C.H. June, A. Natsume, and H. Okada. 2013. Expression of miR-17-92 enhances anti-tumor activity of T-cells transduced with the anti-EGFRvIII chimeric antigen receptor in mice bearing human GBM xenografts. *J. Immunother. Cancer.* 1:21. https://doi.org/10.1186/2051-1426-1-21

Okada, H., G. Kohanbash, X. Zhu, E.R. Kastenhuber, A. Hoji, R. Ueda, and M. Fujita. 2009. Immunotherapeutic approaches for glioma. *Crit. Rev. Immunol.* 29:1–42. https://doi.org/10.1615/CritRevImmunol.v29.i1.10

Okamoto, S., J. Mineno, H. Ikeda, H. Fujiwara, M. Yasukawa, H. Shiku, and I. Kato. 2009. Improved expression and reactivity of transduced tumor-specific TCRs in human lymphocytes by specific silencing of endogenous TCR. *Cancer Res.* 69:9003–9011. https://doi.org/10.1158/0008-5472.CAN-09-1450

Okamoto, S., Y. Amaishi, Y. Goto, H. Ikeda, H. Fujiwara, K. Kuzushima, M. Yasukawa, H. Shiku, and J. Mineno. 2012. A promising vector for TCR gene therapy: Differential effect of siRNA, 2A peptide, and disulfide bond on the introduced TCR expression. *Mol. Ther. Nucleic Acids.* 1:e63. https://doi.org/10.1038/mtna.2012.52

Okano, F., W.J. Storkus, W.H. Chambers, I.F. Pollack, and H. Okada. 2002. Identification of a novel HLA-A*0201-restricted, cytotoxic T lymphocyte epitope in a human glioma-associated antigen, interleukin 13 receptor alpha2 chain. *Clin. Cancer Res.* 8:2851–2855.

Parkhurst, M.R., J.C. Yang, R.C. Langan, M.E. Dudley, D.A. Nathan, S.A. Feldman, J.L. Davis, R.A. Morgan, M.J. Merino, R.M. Sherry, et al. 2011. T cells targeting carcinoembryonic antigen can mediate regression of metastatic colorectal cancer but induce severe transient colitis. *Mol. Ther.* 19:620–626. https://doi.org/10.1038/mt.2010.272

Reardon, D.A., K.W. Wucherpfennig, G. Freeman, C.J. Wu, E.A. Chiocca, P.Y. Wen, W.T. Curry Jr., D.A. Mitchell, P.E. Fecci, J.H. Sampson, and G. Dranoff. 2013. An update on vaccine therapy and other

immunotherapeutic approaches for glioblastoma. *Expert Rev. Vaccines.* 12:597–615. https://doi.org/10.1586/erv.13.41

Rosenberg, S.A., and N.P. Restifo. 2015. Adoptive cell transfer as personalized immunotherapy for human cancer. *Science.* 348:62–68. https://doi.org/10.1126/science.aaa4967

Rosenberg, S.A., R.M. Sherry, K.E. Morton, W.J. Scharfman, J.C. Yang, S.L. Topalian, R.E. Royal, U. Kammula, N.P. Restifo, M.S. Hughes, et al. 2005. Tumor progression can occur despite the induction of very high levels of self/tumor antigen-specific CD8+ T cells in patients with melanoma. *J. Immunol.* 175:6169–6176. https://doi.org/10.4049/jimmunol.175.9.6169

Sasaki, K., X. Zhu, C. Vasquez, F. Nishimura, J.E. Dusak, J. Huang, M. Fujita, A. Wesa, D.M. Potter, P.R. Walker, et al. 2007. Preferential expression of very late antigen-4 on type 1 CTL cells plays a critical role in trafficking into central nervous system tumors. *Cancer Res.* 67:6451–6458. https://doi.org/10.1158/0008-5472.CAN-06-3280

Schroeder, K.M., C.M. Hoeman, and O.J. Becher. 2014. Children are not just little adults: Recent advances in understanding of diffuse intrinsic pontine glioma biology. *Pediatr. Res.* 75:205–209. https://doi.org/10.1038/pr.2013.194

Schumacher, T., L. Bunse, S. Pusch, F. Sahm, B. Wiestler, J. Quandt, O. Menn, M. Osswald, I. Oezen, M. Ott, et al. 2014. A vaccine targeting mutant IDH1 induces antitumour immunity. *Nature.* 512:324–327. https://doi.org/10.1038/nature13387

Schwartzentruber, J., A. Korshunov, X.Y. Liu, D.T. Jones, E. Pfaff, K. Jacob, D. Sturm, A.M. Fontebasso, D.A. Quang, M. Tönjes, et al. 2012. Driver mutations in histone H3.3 and chromatin remodelling genes in paediatric glioblastoma. *Nature.* 482:226–231. https://doi.org/10.1038/nature10833

Sidney, J., S. Southwood, C. Moore, C. Oseroff, C. Pinilla, H.M. Grey, and A. Sette. 2013. Measurement of MHC/peptide interactions by gel filtration or monoclonal antibody capture. *Curr. Protoc. Immunol.* Chatper 18:Unit 18.3. https://doi.org/10.1002/0471142735.im1803s100

Solomon, D.A., M.D. Wood, T. Tihan, A.W. Bollen, N. Gupta, J.J. Phillips, and A. Perry. 2016. Diffuse midline gliomas with histone H3-K27M mutation: A series of 47 cases assessing the spectrum of morphologic variation and associated genetic alterations. *Brain Pathol.* 26:569–580. https://doi.org/10.1111/bpa.12336

Thorne, A.H., C. Zanca, and F. Furnari. 2016. Epidermal growth factor receptor targeting and challenges in glioblastoma. *Neuro-oncol.* 18:914–918. https://doi.org/10.1093/neuonc/nov319

Tran, E., M. Ahmadzadeh, Y.C. Lu, A. Gros, S. Turcotte, P.F. Robbins, J.J. Gartner, Z. Zheng, Y.F. Li, S. Ray, et al. 2015. Immunogenicity of somatic mutations in human gastrointestinal cancers. *Science.* 350:1387–1390. https://doi.org/10.1126/science.aad1253

Tran, E., P.F. Robbins, Y.C. Lu, T.D. Prickett, J.J. Gartner, L. Jia, A. Pasetto, Z. Zheng, S. Ray, E.M. Groh, et al. 2016. T-cell transfer therapy targeting mutant KRAS in cancer. *N. Engl. J. Med.* 375:2255–2262. https://doi.org/10.1056/NEJMoa1609279

Werfel, T., M. Boeker, and A. Kapp. 1997. Rapid expression of the CD69 antigen on T cells and natural killer cells upon antigenic stimulation of peripheral blood mononuclear cell suspensions. *Allergy.* 52:465–469. https://doi.org/10.1111/j.1398-9995.1997.tb01031.x

Wu, G., A. Broniscer, T.A. McEachron, C. Lu, B.S. Paugh, J. Becksfort, C. Qu, L. Ding, R. Huether, M. Parker, et al. St. Jude Children's Research Hospital–Washington University Pediatric Cancer Genome Project. 2012. Somatic histone H3 alterations in pediatric diffuse intrinsic pontine gliomas and non-brainstem glioblastomas. *Nat. Genet.* 44:251–253. https://doi.org/10.1038/ng.1102

Zhang, L., and R.A. Morgan. 2012. Genetic engineering with T cell receptors. *Adv. Drug Deliv. Rev.* 64:756–762. https://doi.org/10.1016/j.addr.2011.11.009

Zhang, A.S., Q.T. Ostrom, C. Kruchko, L. Rogers, D.M. Peereboom, and J.S. Barnholtz-Sloan. 2017. Complete prevalence of malignant primary brain tumors registry data in the United States compared with other common cancers, 2010. *Neuro-oncol.* 19:726–735. https://doi.org/10.1093/neuonc/now252

Zhang, J.G., J. Eguchi, C.A. Kruse, G.G. Gomez, H. Fakhrai, S. Schroter, W. Ma, N. Hoa, B. Minev, C. Delgado, et al. 2007. Antigenic profiling of glioma cells to generate allogeneic vaccines or dendritic cell-based therapeutics. *Clin. Cancer Res.* 13:566–575. https://doi.org/10.1158/1078-0432.CCR-06-1576

Zhu, X., F. Nishimura, K. Sasaki, M. Fujita, J.E. Dusak, J. Eguchi, W. Fellows-Mayle, W.J. Storkus, P.R. Walker, A.M. Salazar, and H. Okada. 2007. Toll like receptor-3 ligand poly-ICLC promotes the efficacy of peripheral vaccinations with tumor antigen-derived peptide epitopes in murine CNS tumor models. *J. Transl. Med.* 5:10. https://doi.org/10.1186/1479-5876-5-10

Zhu, X., B.A. Fallert-Junecko, M. Fujita, R. Ueda, G. Kohanbash, E.R. Kastenhuber, H.A. McDonald, Y. Liu, P. Kalinski, T.A. Reinhart, et al. 2010. Poly-ICLC promotes the infiltration of effector T cells into intracranial gliomas via induction of CXCL10 in IFN-alpha and IFN-gamma dependent manners. *Cancer Immunol. Immunother.* 59:1401–1409. https://doi.org/10.1007/s00262-010-0876-3